JOURNAL
OF
PHYSICS OF THE EARTH

Volume VII - 12 June 1959 - 64 Number 1

CONTENTS

PUBLISHED JOINTLY BY

THE SEISMOLOGICAL SOCIETY OF JAPAN
THE GEODETIC SOCIETY OF JAPAN
THE VOLCANOLOGICAL SOCIETY OF JAPAN

JOURNAL OF PHYSICS OF THE EARTH

The object of the publication of JOURNAL OF PHYSICS OF THE EARTH is to provide an international medium for the publication of original contributions in the field of geophysical science, more particularly concerning with physical properties and conditions of and phenomena occurring in the solid part of the earth.

The JOURNAL is open to any one who wishes to contribute his (or her) article. But the authors are, in principle, requested to pay page charges necessary for publishing their respective articles. The authors receive 100 copies of reprints free of charge.

In order to serve the purposes for which this JOURNAL is published, all contributions should be written in widely understandable languages, such as English, French and German, etc. Contributions should be sent to the Editor or to one of the Associate Editors.

For the time being, this JOURNAL will be issued at variable prices and at irregular intervals. The price of this issue is 200 yen inside Japan and $1.00 for foreign countries, the latter including postage.

Subscriptions may be made through Charles E. Tuttle Co., Booksellers and publishers; Rutland, Vermont, U.S.A. or 15, Edogawa-cho, Bunkyo-ku, Tokyo, Japan.

JOURNAL OF PHYSICS OF THE EARTH, VOL. 7, No. 1, 1959

A Perturbation Method for Studying Thermal Convection Problems

By

Bin OKAI

Geophysical Institute, Faculty of Science, Tokyo University, Tokyo

Abstract

When a layer of fluid is heated uniformly from below, and the Rayleigh number exceeds a critical value, convection takes place in it in a regular cellular pattern. A perturbation method is presented here for determining mathematically the pattern and amplitude of this steady convective motion. The essential point of the method is to expand functions which describe the velocity and temperature field in the fluid in a power series of a parameter ε, while the Rayleigh number is put as a product of the critical value times $(1+\varepsilon^2)$. A set of inhomogeneous equations thus obtained can be solved by the perturbation method which is in use in non-linear oscillation problems. In the two-dimensional case, the slope of heat transport curve becomes steepened abruptly when the Rayleigh numher exceeds a critical value. Another problem which can be dealt with by this method is that of convection within a sphere. This forms an extension of CHANDRASEKHAR's linearized stability theory.

Furthermore, a study is made of the steady thermal convection in a two-dimensional fluid layer when it is heated uniformly from below under a simultaneous constraint of non-uniform temperature given on its upper surface. Mathematically this is an application of the method mentioned above to a problem with inhomogeneous boundary conditions. It was found that the site of spontaneous convection cells is governed by the surface temperature disturbance having a critical wave length. Surface temperature disturbances having much longer or shorter wave lengths play very little part in this, while those having wave lengths close to the critical one have influential effect in determining the general feature of fluid motion.

§ 1. Although the earth's mantle behaves as a solid for forces of short duration such as those occurring in earthquake waves and in earth tides, it may well behave as a fluid for those of very long duration, such as suggested by approximate isostatic adjustments of large topographic features. If this is actually so, there is a possibility that the mantle may be subject to a very slow convection (PEKERIS, 1935; HALES, 1936; BULLARD, 1950). Of course, some difficulties arise in supposing convection currents in the mantle. BIRCH (1951) has pointed out that the currents, if they take place at all, can hardly extend up to the 20° discontinuity. Two recent discoveries appear, however, to support the hypothesis of convection in the mantle. One is concerned with the heat flow from within the earth. The measurements which have been made up to now in this connection (BULLARD, 1954; BULLARD, MAXWELL and REVELLE, 1956; HERZEN, 1959) appear to indicate that the heat flow in oceanic bottoms does not differ significantly from that in continents. The source of heat is reasonably supposed to be due to radioactivity within the crust, which is 35 km thick on the continent and 5 km under the ocean. Where does the oceanic heat come from? If radioactivity is distributed through too great a depth, the temperature near the bottom of the radioactive layer will rise above its melting point, and this is inconsistent with the fact that S waves can be propagated at these depths. This difficulty may be avoided if the transport of heat by convection in the mantle is assumed. The other discovery is concerned with palaeomagnetism. Studies of palaeomagnetism (BLACKETT, 1956; RUNCORN, 1955; CREER, IRVING and RUNCORN, 1954) have rejuvenated interest about the classical hypo-

thesis of continental drifts. But some reasonable forces which drive continental blocks in motion must be looked for if the hypothesis is to become more than a mere hypothesis. Here again, these forces may be assumed to be due to convection currents within the mantle.

Although there are evidences like these in favour of convection currents in the mantle, nothing definite can be said at present about the existence of such large scale motions itself. This is partly because we do not have enough knowledge about the earth and partly because mathematical studies of convection so far developed are far from being satisfactory for the purpose. There are many fundamental problems of thermal convection to be solved. How much heat is transported after convection once takes place in a layer of fluid which so far has been at rest? What would the distribution of temperature become in a convective layer? In 1958, Malkus and Veronis presented a perturbation method by which the form and amplitude of cellular convection can be determined. Their intention was to complete Rayleigh's first-order solution of the problem. At about the same time the present writer found a similar method independently. It was when he had finished his calculations up to §8 of the present article, that he was informed of Malkus and Veronis' paper by Dr. Chandrasekhar of Chicago University (Oct. 24, 1958). A part of the results presented here is similar to those of Malkus and Veronis. In the following, stress will be laid upon the writer's own method of analysis which is more or less different from theirs.

In §2, the fundamental equations and boundary conditions of the problem are stated. In §3, the perturbation method of solutions for the finite amplitude fields of temperature and velocity is described. The method can be applied to other problems, of which a simple example is given. In §4, this method is applied to a two-dimensional convection problem (roll case). In §5, the relation between the heat transport and the mean temperature gradient is studied. In §6, the fundamental equations and boundary conditions are described for the convection within a sphere and in §7, analysis is carried out on this problem. In §8, convective fluid motions which take place within a slowly rotating sphere are considered. Up to this point the boundary conditions are homogeneous. Hereafter inhomogeneous boundary conditions are dealt with. The reason why the inhomogeneity is brought up is as follows. When the temperature difference between the upper and lower surfaces exceeds a certain critical value, convection takes place in a regular cellular pattern, but theory does not distinguish whether horizontal pattern of convection cells is rectangular, triangular or hexagonal. Thus we cannot answer a question such as; Why does one of these patterns take place preferentially, when more than one solution is possible at the point of instability? Even when the motion is taken to be two-dimensional, one cannot predict where the site of upwelling will be located in the fluid. The motion could be upward anywhere, so long as the fluid is uniform horizontally. But such a perfect uniformity cannot be imagined in nature. It is of importance therefore to know the influence of inhomogeneity. Besides, in the case of convection within the earth's mantle, consideration must be paid to the earth's crust of non-uniform thickness. §9 and §10 correspond to §2 and §4 for homogeneous case respectively. In §11 the results obtained are given.

Finally it is admitted that there are many related geophysical problems out of the scope of the new method presented here. This is merely one step toward generalisation of the classical linear stability theory.

§2. First of all, a two-dimensional steady convective motion in a fluid as shown schematically in Fig. 1 will be dealt with. The fluid is supposed to be enclosed between two horizontal conducting surfaces, which are h apart. The lower surface is kept at a temperature T_0 and the upper surface at a lower temperature $(T_0-\beta h)$, the mean temperature gradient being $-\beta$, $(\beta>0)$. The fundamental equations are the equation of continuity (1), the equation of motions of Navier-Stokes (2), (3), the equation of thermal conduction (4)

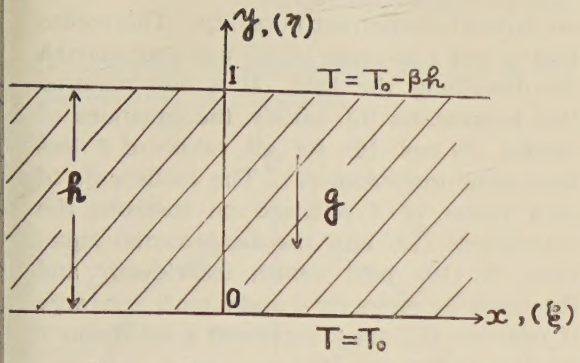

Fig. 1. Fluid layer heated from below.

and the equation of thermal expansion (5):

$$\frac{\partial u}{\partial x}+\frac{\partial v}{\partial y}=0 \tag{1}$$

$$\rho\left(u\frac{\partial u}{\partial x}+v\frac{\partial u}{\partial y}\right)=-\frac{\partial p}{\partial x}+\mu\nabla^2 u \tag{2}$$

$$\rho\left(u\frac{\partial v}{\partial x}+v\frac{\partial v}{\partial y}\right)=-\frac{\partial p}{\partial y}-\rho g+\mu\nabla^2 v \tag{3}$$

$$u\frac{\partial T}{\partial x}+v\frac{\partial T}{\partial y}=\kappa\nabla^2 T \tag{4}$$

$$\rho=\rho_0\{1-\alpha(T-T_0)\}, \tag{5}$$

where u and v are the components of fluid velocity in the direction of x and y respectively, T is the temperature, p is the pressure, g is the magnitude of the gravitational acceleration, μ is the viscosity of the fluid, κ is the thermometric conductivity, ρ is the density, and α the linear coefficient of thermal expansion. Using the stream function ϕ, u and v may be rewritten as $u=\frac{\partial\phi}{\partial y}$ and $v=-\frac{\partial\phi}{\partial x}$.

At this point it is of value to non-dimensionalize the physical quantities appearing in the equations. This will simplify subsequent mathematical manipulations and help us getting pertinent physical parameters for the problem.

Let $$T=\beta h(-y+\tau),\quad x=h\xi,\quad y=h\eta,\quad \phi=\kappa\psi, \tag{6}$$

and after these transformations, all primes will be dropped out. Then (2) and (3) are cross-differentiated and the difference taken in order to have pressure eliminated. The resulting relations between ψ and τ are

$$\frac{\kappa}{\nu}\left[\frac{\partial\psi}{\partial\eta}\left(\frac{\partial^3\psi}{\partial\xi\partial\eta^2}+\frac{\partial^3\psi}{\partial\xi^3}\right)-\frac{\partial\psi}{\partial\xi}\left(\frac{\partial^3\psi}{\partial\eta^3}+\frac{\partial^3\psi}{\partial\xi^2\partial\eta}\right)\right]$$
$$=-R\frac{\partial\tau}{\partial\xi}+\nabla^4\psi \tag{7}$$

$$\frac{\partial\psi}{\partial\eta}\frac{\partial\tau}{\partial\xi}-\frac{\partial\psi}{\partial\xi}\frac{\partial\tau}{\partial\eta}+\frac{\partial\omega}{\partial\xi}=\nabla^2\tau. \tag{8}$$

$R\equiv\frac{\alpha\beta g h^4}{\kappa\nu}$ is a non-dimensional parameter which is called the RAYLEIGH number and $\frac{\nu}{\kappa}$ is the PRANDTL number. So far all the non-linear terms have been retained, but, hereafter, for the sake of simplicity, the inertia terms will be ignored, as it is those non-linear terms appearing in (8) that are more essential in the problem. Also, in the case of convection within the earth's mantle, the inertia terms are negligible because the pertaking viscosity is enormously high. Thus the final equations become

$$\frac{\partial\psi}{\partial y}\frac{\partial\tau}{\partial x}-\frac{\partial\psi}{\partial x}\frac{\partial\tau}{\partial y}+\frac{\partial\psi}{\partial x}=\nabla^2\tau \tag{9}$$

$$\nabla^4\psi=R\frac{\partial\tau}{\partial x}. \tag{10}$$

The conditions at the boundaries ($y=1$, $y=0$) are

$$\frac{\partial\psi}{\partial x}=0,\qquad \frac{\partial^2\psi}{\partial y^2}-\frac{\partial^2\psi}{\partial x^2}=0,\quad \tau=0, \tag{11}$$

following RAYLEIGH. This means that temperatures are kept constant, the vertical component of velocity vanishes and stress does not exist at the boundaries. In other words, the boundaries are free. More realistic are of course the conditions of 'rigid-rigid' or 'rigid-free', but these are difficult to be taken into account. Essential points of the problem are not lost by adopting the above-mentioned unrealistic conditions.

§ 3. A convective motion takes place in the fluid layer when the mean temperature gradient β (or R) reaches a critical value β_0 (or R_0). A further increase of mean temperature gradient produces more intense field of motion. Therefore functions ψ and τ describing the

field must appear suddenly when β reaches β_0. In other words, ψ and τ are not analytic at $\beta=\beta_0$ (Fig. 2). Consequently one cannot expect solutions in the form

$$\left.\begin{aligned}&\beta=\beta_0(1+\delta)\\&\psi=\delta\cdot\psi_1+\delta^2\cdot\psi_2+\delta^3\cdot\psi_3+\cdots\\&\tau=\delta\cdot\tau_1+\delta^2\cdot\tau_2+\delta^3\cdot\tau_3+\cdots\end{aligned}\right\}\qquad(12)$$

which are all analytic. If ψ and τ could be written in the form mentioned above, ψ and τ could be extended to include the state having the temperature gradient less than the critical one, and this will mean that a convective motion could occur even before the mean temperature gradient β reaches the critical value β_0. This is absurd and does not represent actual cases. Therefore another form of solutions has to be looked for. The weakest point of the expression $\beta=\beta_0(1+\delta)$ in (12) is that β can easily become less than β_0, while physically δ must always be positive. This can be avoided if δ is put to be equal to ε^2. But if all the δ's in (12) are made equal to ε^2, the situation will still be the same, for there is no reason to suppose that ε does not

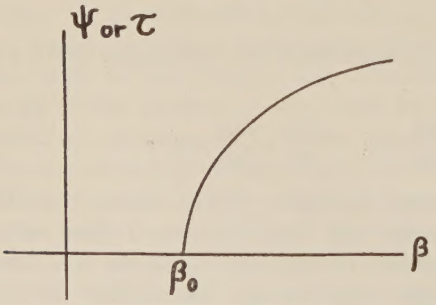

Fig. 2. Relation between mean temp. grad. and the function describing the field. ψ, (τ) is not analytic at the point where $\beta=\beta_0$.

become imaginary and the absurdity remains. The difficulties will disappear if one could find solutions in the following form

$$\left.\begin{aligned}&\beta=\beta_0(1+\varepsilon^2)\\&\psi=\varepsilon\psi_1+\varepsilon^2\psi_2+\varepsilon^3\psi_3+\cdots\\&\tau=\varepsilon\tau_1+\varepsilon^2\tau_2+\varepsilon^3\tau_3+\cdots\end{aligned}\right\}.\qquad(13)$$

Of course, here again β becomes less than β_0 if ε is taken as pure imaginary. But ψ and τ, then, become complex functions which have no physical counterpart in reality. This means that ψ and τ as given in (13) are good enough for describing the field. It is now required that expressions (13) satisfy the equations of motion, (9) and (10), for all values of ε less than some maximum ε_m. The coefficients of each power of ε obtained on inserting the expressions (13) into the fundamental equations (9), (10) must vanish individually and the resulting series for ψ and τ must converge if relations (13) are to represent a satisfactory solution to the problem.

The sequence of linear inhomogeneous equations in powers of ε obtained on inserting relations (13) into equations (9) and (10) is

$$\Delta^4\sum_i\varepsilon^i\psi_i=R_0(1+\varepsilon^2)\frac{\partial}{\partial x}\sum_i\varepsilon^i\tau_i\qquad(14)$$

$$\frac{\partial}{\partial y}\sum_i\varepsilon^i\psi_i\frac{\partial}{\partial x}\sum_i\varepsilon^i\tau_i-\frac{\partial}{\partial x}\sum_i\varepsilon^i\psi_i\frac{\partial}{\partial y}\sum_i\varepsilon^i\tau_i+\frac{\partial}{\partial x}\sum_i\varepsilon^i\psi_i=\nabla^2\sum_i\varepsilon^i\tau_i\,.\qquad(15)$$

Using ψ and τ, the original quantities u, v and T are expressed as follows:

$$u=\frac{\kappa}{h}\frac{\partial\psi}{\partial y},\quad v=-\frac{\kappa}{h}\frac{\partial\psi}{\partial x},\quad T=h\beta_0(1+\varepsilon^2)(-y+\tau),\qquad(16)$$

where x and y are non-dimensional.

The expansion method described here is also applicable to other problems, in which dependent variables are single-valued and the domain of these variables is bounded. As a simple example, the problem of one-dimensional simple harmonic oscillator is dealt with. The governing equation with regard to the velocity v is

$$v\frac{dv}{dx}+\omega^2x=0\,,\qquad(17)$$

which, of course, can be integrated easily. But here, the above-mentioned method of expansion is followed. In (17), x is upper-bounded and has some maximum value, a (amplitude of oscillator), as shown in Fig. 3. The situation near $x=a$ (or $x=-a$) in Fig. 3 is quite the same as the neighbourhood of $\beta=\beta_0$ in Fig. 2. Therefore v and x are put as

$$x=a-\varepsilon^2,\quad v=A_1\varepsilon+A_2\varepsilon^2+A_3\varepsilon^3+\cdots.\qquad(18)$$

By changing the independent variable in (17) from x to ξ, (17) becomes

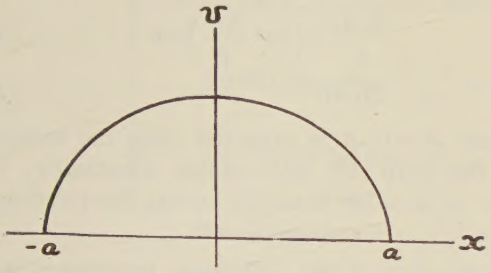

Fig. 3. Relation between velocity and displacement of a linear oscillator. v is not analytic where $x=\pm a$.

$$-\frac{v}{2\xi}\frac{dv}{d\xi}+\omega^2(a-\xi^2)=0\,. \tag{19}$$

Explicit determination of A_i's need not be mentioned, as it is quite elementary. Finally it is shown that the solution thus obtained is no other than $\frac{1}{2}v^2+\frac{\omega^2}{2}x^2=E$.

§ 4. In this section, the sequence of equations, (14), (15) will be solved.

[ε]: The first-order equations are

$$\nabla^4\psi_1=R_0\frac{\partial\tau_1}{\partial x} \tag{20}$$

$$\frac{\partial\psi_1}{\partial x}=\nabla^2\tau_1\,. \tag{21}$$

These are concerned with the stability theory and have been exactly solved in terms of trigonometric functions (Rayleigh, 1916). A complete solution is

$$\psi_1=A_1\sin\pi y\sin\frac{\pi}{\sqrt{2}}x \tag{22}$$

$$\tau_1=-\frac{\sqrt{2}A_1}{3\pi}\sin\pi y\cos\frac{\pi}{\sqrt{2}}x \tag{23}$$

$$R_0=\frac{27}{4}\pi^4\,. \tag{24}$$

This is obtained by assuming a solution in the form $e^{im\pi x}\sin n\pi y$ and then making the value of R (or the mean temperature gradient) as small as possible. Thus $R_0=\underset{m,\,n\ \text{(integer)}}{\text{Min}}\,R(m,n)$, where n is an integer. An explicit value of A_1 in (22) and (23) will be obtained in the third-order stage [ε^3]. Finally it is noted at this point that the origin of the coordinates is so chosen as to make $u=0$ at $x=0$.

[ε^2]:
$$\nabla^4\psi_2=R_0\frac{\partial\tau_2}{\partial x} \tag{25}$$

$$\frac{\partial\psi_1}{\partial y}\frac{\partial\tau_1}{\partial x}-\frac{\partial\psi_1}{\partial x}\frac{\partial\tau_1}{\partial y}+\frac{\partial\psi_2}{\partial x}=\nabla^2\tau_2 \tag{26}$$

Inserting (22) and (23) into (25) and (26) and solving the equations thus obtained, we get the following solution to the second-order equations:

$$\psi_2=A_2\sin\pi y\sin\frac{\pi}{\sqrt{2}}x \tag{27}$$

$$\tau_2=-\frac{\sqrt{2}A_2}{3\pi}\sin\pi y\cos\frac{\pi}{\sqrt{2}}x-\frac{{A_1}^2}{24\pi}\sin 2\pi y. \tag{28}$$

Here again, the solution contains a new arbitrary constant A_2, which is determined explicitly in a later stage.

[ε^3]:
$$\nabla^4\psi_3=R_0\frac{\partial\tau_3}{\partial x}+R_0\frac{\partial\tau_1}{\partial x} \tag{29}$$

$$\frac{\partial\psi_1}{\partial y}\frac{\partial\tau_2}{\partial x}+\frac{\partial\psi_2}{\partial y}\frac{\partial\tau_1}{\partial x}-\frac{\partial\psi_1}{\partial x}\frac{\partial\tau_2}{\partial y}-\frac{\partial\psi_2}{\partial x}\frac{\partial\tau_1}{\partial y}+\frac{\partial\psi_3}{\partial x}=\nabla^2\tau_3 \tag{30}$$

Inserting (22), (23), (27) and (28) into (29) and (30), we get the following equation:

$$\nabla^6\psi_3-R_0\frac{\partial^2\psi_3}{\partial x^2}=\frac{R_0\pi^2}{2}A_1\left(\frac{{A_1}^2}{24}-1\right)\sin\pi y\sin\frac{\pi}{\sqrt{2}}x$$
$$-R_0\frac{{A_1}^3\pi}{48}\sin 3\pi y\sin\frac{\pi}{\sqrt{2}}x. \tag{31}$$

On the right hand side of (31) there are two inhomogeneous terms. The one which has the form of $\sin\pi y\sin\frac{\pi}{\sqrt{2}}x$ will generate a particular integral which does not satisfy the boundary conditions. Therefore we have to choose the value of A_1 so as to eliminate the resonant inhomogeneous term in (31), (a method used in non-linear-oscillation problems):

$$\frac{R_0\pi^2}{2}A_1\left(\frac{{A_1}^2}{24}-1\right)=0 \tag{32}$$

$$A_1=\sqrt{24},\quad -\sqrt{24},\quad 0 \tag{33}$$

Thus the determination of A_1 has been made which was impossible in the earlier stage of

$[\varepsilon]$. Of the three values in (33), $-\sqrt{24}$ is discarded as it coincides with $\sqrt{24}$ by another choice of coordinates. Also $A_1=0$ must be discarded. This represents no other than the state of unstable rest.

$$[\varepsilon^4]: \qquad \nabla^4\psi_4=R_0\frac{\partial\tau_4}{\partial x}+R_0\frac{\partial\tau_2}{\partial x} \tag{34}$$

$$\frac{\partial\psi_1}{\partial y}\frac{\partial\tau_3}{\partial x}+\frac{\partial\psi_2}{\partial y}\frac{\partial\tau_2}{\partial x}+\frac{\partial\psi_3}{\partial y}\frac{\partial\tau_1}{\partial x}-\frac{\partial\psi_1}{\partial x}\frac{\partial\tau_3}{\partial y}-\frac{\partial\psi_2}{\partial x}\frac{\partial\tau_2}{\partial y}-\frac{\partial\psi_3}{\partial x}\frac{\partial\tau_1}{\partial y}+\frac{\partial\psi_4}{\partial x}=\nabla^2\tau_4 \tag{35}$$

Rearranging the equations into a single one and eilminating the resonant inhomogeneous term, we get the following relation as in case of $[\varepsilon^3]$:

$$\frac{R_0A_2}{2}\pi^2\left(1-\frac{A_1^2}{8}\right)=0\,. \tag{36}$$

$$\therefore\quad A_2=0 \tag{37}$$

From $A_2=0$, it is expected that the solution in the form (12) will vanish identically, for (12) is no other than (13) having the relations: $\psi_1=\psi_3=\cdots=\tau_1=\tau_3=\cdots=0$.

Explanation of the following procedures will not be necessary. The results are just written down up to the stage of $[\varepsilon^7]$:

$$[\varepsilon]\quad\begin{cases}\psi_1=4.898\sin\pi y\sin\dfrac{\pi}{\sqrt{2}}x\\ \tau_1=-0.735\sin\pi y\cos\dfrac{\pi}{\sqrt{2}}x\end{cases}$$

$$[\varepsilon^2]\quad\begin{cases}\psi_2=0\\ \tau_2=-0.318\sin 2\pi y\end{cases}$$

$$[\varepsilon^3]\quad\begin{cases}\psi_3=0.385\sin\pi y\sin\dfrac{\pi}{\sqrt{2}}x+0.019\sin 3\pi y\sin\dfrac{\pi}{\sqrt{2}}x\\ \tau_3=0.675\sin\pi y\cos\dfrac{\pi}{\sqrt{2}}x-0.116\sin 3\pi y\cos\dfrac{\pi}{\sqrt{2}}x\end{cases}$$

$$[\varepsilon^4]\quad\begin{cases}\psi_4=-0.058\sin 2\pi y\sin\sqrt{2}\,\pi x+0.001\sin 4\pi y\sin\sqrt{2}\,\pi x\\ \tau_4=0.320\sin 2\pi y-0.025\sin 4\pi y+0.070\sin 2\pi y\cos\sqrt{2}\,\pi x\\ \qquad -0.011\sin 4\pi y\cos\sqrt{2}\,\pi x\end{cases}$$

$$[\varepsilon^5]\quad\begin{cases}\psi_5=-0.130\sin\pi y\sin\dfrac{\pi}{\sqrt{2}}x+0.070\sin\pi y\sin\dfrac{3\sqrt{2}}{2}\pi x-0.006\sin 3\pi y\sin\dfrac{\pi}{\sqrt{2}}x\\ \qquad -0.001\sin 3\pi y\sin\dfrac{3\sqrt{2}}{2}\pi x\\ \tau_5=-0.666\sin\pi y\cos\dfrac{\pi}{\sqrt{2}}x-0.047\sin\pi y\cos\dfrac{3\sqrt{2}}{2}\pi x+0.157\sin 3\pi y\cos\dfrac{\pi}{\sqrt{2}}x\\ \qquad +0.004\sin 3\pi y\cos\dfrac{3\sqrt{2}}{2}\pi x-0.009\sin 5\pi y\cos\dfrac{\pi}{\sqrt{2}}x\end{cases}$$

$$[\varepsilon^6]\quad\begin{cases}\psi_6=A_6\sin\pi y\sin\dfrac{\pi}{\sqrt{2}}x+0.041\sin 2\pi y\sin\sqrt{2}\,\pi x-0.014\sin 2\pi y\sin 2\sqrt{2}\,\pi x\\ \qquad -0.001\sin 4\pi y\sin\sqrt{2}\,\pi x.\\ \tau_6=-0.323\sin 2\pi y+0.034\sin 4\pi y-0.001\sin 6\pi y-0.1500A_6\sin\pi y\cos\dfrac{\pi}{\sqrt{2}}x\\ \qquad -0.119\sin 2\pi y\cos\sqrt{2}\,\pi x+0.005\sin 2\pi x\cos 2\sqrt{2}\,\pi x\\ \qquad +0.017\sin 4\pi y\cos\sqrt{2}\,\pi x+0.001\sin 4\pi y\cos 2\sqrt{2}\,\pi x\end{cases}$$

$$[\varepsilon^7]\quad \begin{cases} \psi_7 = A_7 \sin \pi y \sin \dfrac{\pi}{\sqrt{2}} x - 0.020 \sin \pi y \sin \dfrac{3\sqrt{2}}{2} \pi x + 0.003 \sin 3\pi y \sin \dfrac{\pi}{\sqrt{2}} x \\ \tau_7 = -0.130 A_6 \sin 2\pi y + (0.666 - 0.1500 A_7) \sin \pi y \cos \dfrac{\pi}{\sqrt{2}} x \\ \qquad + 0.061 \sin \pi y \cos \dfrac{3\sqrt{2}}{2} \pi x - 0.001 \sin \pi y \cos \dfrac{5\sqrt{2}}{2} \pi x \\ \qquad - 0.176 \sin 3\pi y \cos \dfrac{\pi}{\sqrt{2}} x - 0.001 \sin 3\pi y \cos \dfrac{3\sqrt{2}}{2} \pi x \\ \qquad + 0.013 \sin 5\pi y \cos \dfrac{\pi}{\sqrt{2}} x + 0.001 \sin 5\pi y \cos \dfrac{3\sqrt{2}}{2} \pi x \end{cases} \tag{38}$$

Explicit determination of A_6 and A_7 has not yet been made, though A_6 is expected to vanish. (38) is rewritten to show the coefficient of each trigonometric function in a power series of ε:

ψ: $\sin \pi y \sin \dfrac{\pi}{\sqrt{2}} x$: $4.898\varepsilon + 0.385\varepsilon^3 - 0.130\varepsilon^5 + A_6\varepsilon^6 + A_7\varepsilon^7$

$\sin \pi y \sin \dfrac{3\pi}{\sqrt{2}} x$: $0.070\varepsilon^5 - 0.020\varepsilon^7$

$\sin 2\pi y \sin \sqrt{2}\,\pi x$: $-0.058\varepsilon^4 + 0.041\varepsilon^6$

$\sin 2\pi y \sin 2\sqrt{2}\,\pi x$: $-0.014\varepsilon^6$

$\sin 3\pi y \sin \dfrac{\pi}{\sqrt{2}} x$: $0.019\varepsilon^3 - 0.006\varepsilon^5 + 0.003\varepsilon^7$

$\sin 3\pi y \sin \dfrac{3\pi}{\sqrt{2}} x$: $-0.001\varepsilon^5$

$\sin 4\pi y \sin \sqrt{2}\,\pi x$: $0.001\varepsilon^4 - 0.005\varepsilon^6$

τ: $\sin 2\pi y$: $-0.318\varepsilon^2 + 0.320\varepsilon^4 - 0.323\varepsilon^6 - 0.130A^6\varepsilon^7$

$\sin 4\pi y$: $-0.025\varepsilon^4 + 0.034\varepsilon^6$

$\sin 6\pi y$: $-0.001\varepsilon^6$

$\sin \pi y \cos \dfrac{\pi}{\sqrt{2}} x$: $-0.735\varepsilon + 0.675\varepsilon^3 - 0.666\varepsilon^5 - 0.1500A_1{}^6$
$+ (0.666 - 0.1500A_7)\varepsilon^7$

$\sin \pi y \cos \dfrac{3\pi}{\sqrt{2}} x$: $-0.047\varepsilon^5 + 0.061\varepsilon^7$

$\sin \pi x \cos \dfrac{5\pi}{\sqrt{2}} x$: $-0.001\varepsilon^7$

$\sin 2\pi y \cos \sqrt{2}\,\pi x$: $0.070\varepsilon^4 - 0.119\varepsilon^6$

$\sin 2\pi y \cos 2\sqrt{2}\,\pi x$: $0.005\varepsilon^6$

$\sin 3\pi y \cos \dfrac{\pi}{\sqrt{2}} x$: $-0.116\varepsilon^3 + 0.157\varepsilon^5 - 0.176\varepsilon^7$

$\sin 3\pi y \cos \dfrac{3\pi}{\sqrt{2}} x$: $0.004\varepsilon^5 - 0.001\varepsilon^7$

$\sin 4\pi y \cos \sqrt{2}\,\pi x$: $-0.011\varepsilon^4 + 0.017\varepsilon^6$

$$\sin 4\pi y \cos 2\sqrt{2}\,\pi x: \quad 0.001\varepsilon^4$$

$$\sin 5\pi y \cos \frac{\pi}{\sqrt{2}} x: \quad -0.009\varepsilon^5 - 0.013\varepsilon^7$$

$$\sin 5\pi y \cos \frac{3\pi}{\sqrt{2}} x: \quad 0.001\varepsilon^7 \ .$$

§ 5. The heat transport increased by convection is easily calculated from the temperature gradient at the boundaries:

$$\text{Heat flow} = -k\frac{d\bar{T}}{d(hy)}_{y=0} = k\beta_0(1+\varepsilon^2)\left(1-\frac{d\bar{\tau}}{dy}\right)_{y=0}$$
$$= k\beta_0(1+\varepsilon^2)(1+1.99\varepsilon-1.70\varepsilon^2+1.61\varepsilon^3-\cdots) \tag{39}$$

where the bars above T and τ denote an average over a horizontal line. Fig. 4 shows the relation between the heat transport and the mean temperature gradient. As an illustration of convective patterns, isothermals and velocity vectors of the fluid are shown in Fig. 5, when the mean temperature gradient is 10% in excess of the critical value. The whole feature changes a little when the mean temperature gradient is 40% in excess of the critical value (Fig. 6).

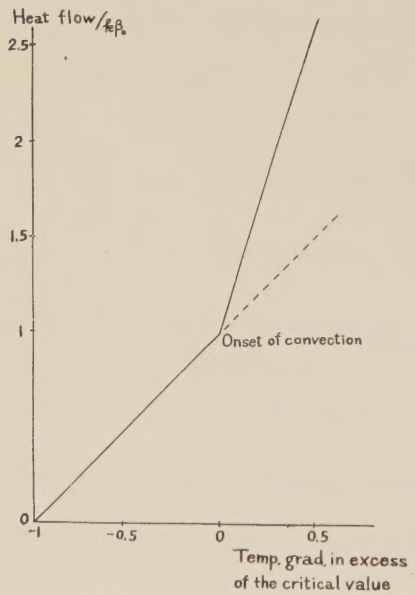

Fig. 4. Heat transport vs. temp. grad.. Dashed line represents the relation due to conduction alone.

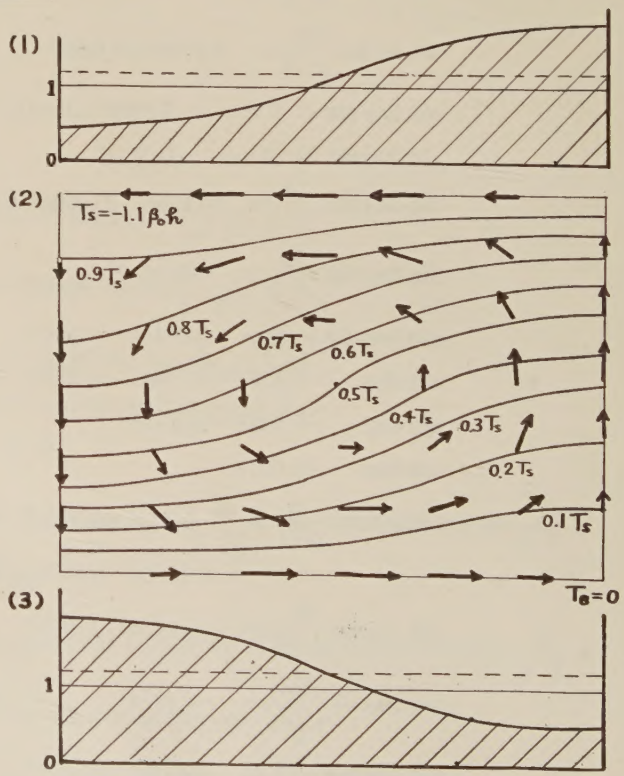

Fig. 5. Mean temp. grad. is 10% in excess of the critical value.
(1) Heat transported from above. Unit of the ordinate is the value due to conduction alone. Dashed line is the averaged value.
(2) Temperature and velocity distribution within a half of the cell. T_S and T_B are temperatures of the surface and the bottom respectively.
(3) Heat transported from below.

§ 6. Unless the fluid motion is restricted to two-dimensional, an infinite number of steady finite amplitude solutions (having different horizontal plan-forms) are obtained which formally satisfy the equations.

Another case which also gives a unique solution as in the roll case is convection

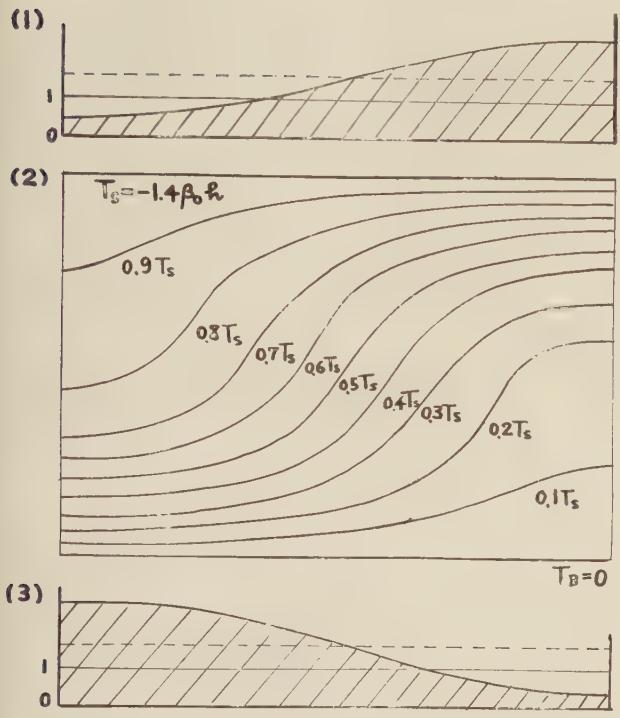

Fig. 6. Mean temp. grad. is 40% in excess of the critical value (cf. Fig. 5).

within a sphere. The following is an extension of CHANDRASEKHAR's linearized stability theory (1952).

Following CHANDRASEKHAR, the sphere is taken to be a homogeneous one of radius R in equilibrium under its own gravitation and with a uniform distribution of heat sources such that in the absence of conduction the temperature at each point will rise at a rate of Q. In the steady state, the temperature distribution, $\bar{T}(r)$, inside the sphere will be governed by

$$\kappa\nabla^2\bar{T}=-Q \tag{40}$$

The solution of (40) appropriate to the problem on hand is

$$\bar{T}=\beta(R^2-r^2),\quad \beta=\frac{Q}{6\kappa}\ . \tag{41}$$

In writing the solution in the form (41), we have assumed that $T=0$ at $r=R$; this entails no loss of generality. Let the temperature distribution in the convective state be given by $T=\bar{T}+\tau$. The equation governing τ is

$$-2\beta\vec{u}\cdot\vec{r}+\vec{u}\cdot\operatorname{grad}\tau=\kappa\nabla^2\tau\ . \tag{42}$$

In (42), the non-linear terms have been retained. Other equations governing the field are

$$\operatorname{div}\vec{u}=0, \tag{43}$$

$$0=-\operatorname{grad}p-\rho\operatorname{grad}V+\rho\nu\nabla^2\vec{u}, \tag{44}$$

where the external field $\operatorname{grad}V$ is that due to the action of gravity in a homogeneous sphere,

$$\operatorname{grad}V=\frac{4}{3}\pi\rho_0 G\vec{r}. \tag{45}$$

G denotes the constant of gravitation and ρ_0 is the mean density.

By replacing ρ by $\rho=\bar{\rho}(1-\alpha T)$, we get from (44)

$$0=-\operatorname{grad}\tilde{\omega}+\gamma\tau\vec{r}++\nu\nabla^2\vec{u} \tag{46}$$

where

$$\left.\begin{aligned}\tilde{\omega}&=\frac{p}{\rho}-V-\frac{1}{4}\beta\gamma(2R^2r^2-r^4)\\ \gamma&=\frac{4}{3}\pi\bar{\rho}G\alpha.\end{aligned}\right\} \tag{47}$$

The physical quantities appearing in the above equations are non-dimensionalized as in § 2:

$$\tau=\beta R^2\tau',\ u=\frac{\kappa}{R}\vec{u}',\ \vec{r}=R\vec{r}'. \tag{48}$$

After these transformations all primes will be dropped out. The following are the fundamental equations in this problem:

$$\operatorname{div}\vec{u}=0 \tag{49}$$

$$-2\vec{r}\cdot\vec{u}+\vec{u}\cdot\operatorname{grad}\tau=\nabla^2\tau \tag{50}$$

$$0=-\operatorname{grad}\tilde{\omega}+\frac{C}{2}\vec{r}\tau+\nabla^2\vec{u} \tag{51}$$

where $C\equiv\dfrac{2\beta\gamma R^5}{\kappa\nu}$.

C corresponds to the RAYLEIGH number R in § 2. After eliminating $\tilde{\omega}$ from (51), we get

$$\nabla^4(ru)+\frac{C}{2}L^2\tau=0 \tag{52}$$

where $L^2=\left\{r^2\nabla^2-r\frac{\partial}{\partial r}-r\frac{\partial}{\partial r}r\frac{\partial}{\partial r}\right\}$

$$=\frac{1}{\sin^2\theta}\frac{\partial}{\partial\theta}\sin\theta\frac{\partial}{\partial\theta}+\frac{1}{\sin^2\theta}\frac{\partial^2}{\partial\varphi^2} \tag{53}$$

and $\vec{u}=(u, v, w,)$ are the components of velocity in the spherical polar coordinates.

On the spherical boundary surface ($r=1$), it is required

1) that the surface temperature is fixed:

$$\tau=0 \tag{54}$$

which, using (52), becomes $\nabla^4(ru)=0$, (55)

2) that u vanishes identically: $ru=0$, (56)

and

3) that, in case of a rigid surface, from the equation of continuity

$$\frac{\partial}{\partial r}(ru)=0\ , \tag{57}$$

or, in case of a free surface, also from the equation of continuity

$$\frac{\partial^2}{\partial r^2}(ru)=0\ . \tag{58}$$

But either of these conditions (57) and (58) makes following calculations extremely difficult. Even in case of the linear stability problem, tedious procedures of variational method are necessary. Therefore, for the sake of simplicity, we impose the following artificial conditions:

$$p_{r\theta}=\rho\nu\left(\frac{\partial u}{r\partial\theta}-\frac{v}{r}+\frac{\partial v}{\partial r}\right)=-\frac{2\rho\nu}{r}v \tag{59}$$

$$p_{r\varphi}=\rho\nu\left(\frac{\partial u}{r\sin\theta\partial\varphi}-\frac{w}{r}+\frac{\partial w}{\partial r}\right)=-\frac{2\rho\nu}{r}w \tag{60}$$

These are reduced respectively to

$$\left(\frac{\partial}{\partial r}+\frac{1}{r}\right)v=0 \tag{61}$$

$$\left(\frac{\partial}{\partial r}+\frac{1}{r}\right)w=0. \tag{62}$$

Using the equation of continuity, (61) and (62) become

$$\nabla^2(ru)=0. \tag{63}$$

From (59) and (60) it is seen that (63) is a condition between 'rigid' and 'free', which is also verified from (72) in § 7.

To sum up, the boundary conditions are (55), (56) and (63).

§ 7. The perturbation method used in this section is quite similar to that used in § 3 and the solution is expected to be expanded in the following form

$$\left.\begin{aligned} &C=C_0(1+\varepsilon^2)\\ &\vec{u}=\varepsilon\vec{u}_1+\varepsilon^2\vec{u}_2+\varepsilon^3\vec{u}_3+\cdots\\ &\tau=\varepsilon\tau_1+\varepsilon^2\tau_2+\varepsilon^3\tau_3+\cdots \end{aligned}\right\} \tag{64}$$

where C_0 is the critical value of C and corresponds to the critical intensity Q_0 of heat sources.

Inserting (64) into (50) and (52) we get a sequence of linear inhomogeneous equations in powers of ε. The following procedures are quite the same as in § 4.

[ε]: The first-order equation is

$$\nabla^6(ru_1)=C_0L^2(ru_1). \tag{65}$$

Now we may assume for the solution of (65) the following form

$$ru_1=W_1(r)Y(\theta, \varphi), \tag{66}$$

where Y is the spherical harmonic of the first order, as the lowest order gives C the least value. The equation for $W_1(r)$ becomes

$$\left[\frac{d^2}{dr^2}+\frac{2}{r}\frac{d}{dr}-\frac{2}{r^2}\right]^3W_1+2C_0W_1=0. \tag{67}$$

The boundary conditions on the surface ($r=1$) are

i) $W_1=0$ (68)

ii) $\left[\frac{d^2}{dr^2}+\frac{2}{r}\frac{d}{dr}-\frac{2}{r^2}\right]W_1=0$ (69)

iii) $\left[\frac{d^2}{dr^2}+\frac{2}{r}\frac{d}{dr}-\frac{2}{r^2}\right]^2W_1=0.$ (70)

Without difficulties the solution of (67) is obtained:

$$W_1=A_1\frac{J_{3/2}(\alpha_1 r)}{\sqrt{r}}\ , \tag{71}$$

where α_1 is the minimum value of α_i's which satisfy $J_{3/2}(\alpha_i)=0$.

Thus C_0 becomes $C_0=\frac{{\alpha_1}^6}{2}=4115.48.$ (72)

According to CHANDRASEKHAR C_0 is 3091.4 in case of the free surface and 8047.1 in case of the rigid one. Therefore, in this respect too, it is seen that (63) represents a condition between 'rigid' and 'free'. From (66) and (71) ru_1 becomes

$$ru_1 = A_1 \frac{J_{3/2}(\alpha_1 r)}{\sqrt{r}} Y_1(\theta_1 \varphi) \,. \tag{73}$$

Explicit value of A_1 in (73) is still unknown and is determined in the third stage [ε^3]. In addition to A_1 there are in fact two more arbitrary constants a_1, b_1, contained in $Y_1(\theta, \varphi)$, for $Y_1(\theta, \varphi) = \cos\theta + a_1 \sin\theta \sin\varphi + b_1 \sin\theta \cos\varphi$. But these will vanish when the axis $\theta = 0$ is chosen artificially to be parallel to the flow at the origin. The situation, however, changes if the sphere is rotating. Later on, it is shown that the above-mentioned direction of motion is decided in regard to the rotating axis.

From
$$-2ru_1 = \nabla^2 \tau_1 \tag{74}$$
τ_1 is derived as
$$\tau_1 = \frac{2A_1}{\alpha_1^2} \frac{J_{3/2}(\alpha_1 r)}{\sqrt{r}} Y_1(\theta, \varphi). \tag{75}$$

The procedure to obtain v and w is as follows. In general, $\vec{u}$ is expressed in the following form;

$$\begin{pmatrix} ru \\ rv \\ rw \end{pmatrix} = \begin{pmatrix} (nF_{m.n} + r^2 G_{n,m}) W_{n,m} \\ F_{m.n} \dfrac{\partial W_{n,m}}{\partial \theta} \\ F_{n,m} \dfrac{1}{\sin\theta} \dfrac{\partial W_{n,m}}{\partial \varphi} \end{pmatrix} + \begin{pmatrix} 0 \\ r \dfrac{L_{n,m}}{\sin\theta} \dfrac{\partial W_{m.n}}{\partial \varphi} \\ -r L_{n,m} \dfrac{\partial W_{n.m}}{\partial \theta} \end{pmatrix} \tag{76}$$

where F, G and L are unknown functions and $W_{n,m} = r^n Y_{n,m}(\theta, \varphi)$. First of all, $L = 0$, as easily seen from (76) and (51). Then the three unknowns are reduced to two (F and G). By an appropriate choice of a harmonic $W_{n,m}$,

these two are determined from (73); $$(F + r^2 G) r = A_1 \frac{J_{3/2}(\alpha_1 r)}{\sqrt{r}} \tag{77}$$

and from the equation of continuity; $$\frac{1}{r} \frac{dF}{dr} + r \frac{dG}{dr} + 4G = 0 \tag{78}$$

as $$G = \frac{A_1 \alpha_1 J_{5/2}(\alpha_1 r)}{2r^{5/2}}, \qquad F = \frac{A_1 J_{3/2}(\alpha_1 r)}{r^{3/2}} - \frac{A_1 \alpha_1 J_{5/2}(\alpha_1 r)}{2r^{1/2}} \,. \tag{79}$$

The final forms of v_1 and w_1 are $$v_1 = A_1 \left[\frac{J_{3/2}(\alpha_1 r)}{r^{3/2}} - \frac{\alpha_1}{2} \frac{J_{5/2}(\alpha_1 r)}{r^{1/2}} \right] \frac{\partial Y_1(\theta, \varphi)}{\partial \theta} \tag{80}$$

$$w_1 = 0 \,. \tag{81}$$

The general pattern of motion is shown in Fig. 7.

[ε^2] The second-order equation is

$$\nabla^6 (ru_2) - C_0 L^2 (ru_2) + \frac{C_0}{2} L^2 (\vec{u_1} \cdot \operatorname{grad} \tau_1) = 0 \tag{82}$$

where $\vec{u_1} \cdot \operatorname{grad} \tau_1$ is

$$\frac{2A_1^2}{3\alpha_1^2} \frac{J_{3/2}(\alpha_1 r)}{r^{3/2}} \left[\frac{d}{dr} \left\{ \frac{J_{3/2}(\alpha_1 r)}{\sqrt{r}} \right\} - \frac{J_{3/2}(\alpha_1 r)}{r^{3/2}} \right] P_2(\cos\theta)$$
$$+ \frac{2A_1 A_2}{3\alpha_1^2} \frac{J_{3/2}(\alpha_1 r)}{r^{3/2}} \left[2 \frac{d}{dr} \left\{ \frac{J_{3/2}(\alpha_1 r)}{\sqrt{r}} \right\} + \frac{J_{3/2}(\alpha_1 r)}{r^{3/2}} \right] \tag{83}$$

The complete solution to the second-order equations is

$$u_2 = A_2 \frac{J_{3/2}(\alpha_1 r)}{r^{3/2}} \cos\theta + 0.12 A_1^2 \frac{J_{5/2}(\beta_1 r)}{r^{3/2}} P_2(\theta) + \cdots$$

$$v_2 = -A_2 \left[\frac{J_{3/2}(\alpha_1 r)}{r^{3/2}} - \frac{\alpha_1}{2} \frac{J_{5/2}(\alpha_1 r)}{\sqrt{r}} \right] \sin\theta - A_1^2 \left[0.09 \frac{J_{5/2}(\beta_1 r)}{r^{3/2}} \right.$$

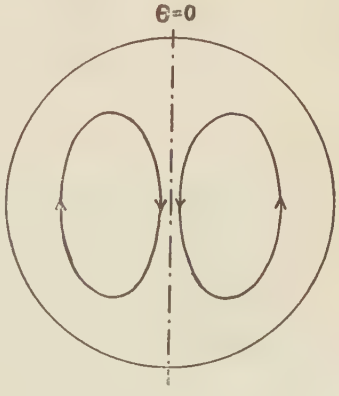

Fig. 7. General pattern of motion $\vec{u_1}$.

$$+0.03r^2\frac{d}{dr}\left\{\frac{J_{5/2}(\beta_1 r)}{r^{5/2}}\right\}\Big]\sin 2\theta+\cdots \tag{84}$$

$$w_2=0$$

$$\tau_2=\frac{2A_2}{\alpha_1^2}\frac{J_{3/2}(\alpha_1 r)}{\sqrt{r}}\cos\theta+0.011A_1^2\frac{J_{5/2}(\beta_1 r)}{\sqrt{r}}P_2(\theta)-0.0067A_1^2\frac{J_{1/2}(\pi r)}{\sqrt{r}}$$

$$-0.0043A_1^2\frac{J_{1/2}(2\pi r)}{\sqrt{r}}+\cdots,$$

where $J_{5/2}(\beta_n)=0$, $(n=1, 2\cdots)$.

[ε^3]: The third-order equation is

$$\nabla^4(ru_3)-C_0L^2(ru_3)+\frac{C_0}{2}L^2[\nabla^2\tau_1+\vec{u}_1\cdot\operatorname{grad}\tau_2+\vec{u}_2\operatorname{grad}\tau_1]=0. \tag{85}$$

In (85), the inhomogeneous term which has the form of $\frac{J_{3/2}(\alpha_1 r)}{\sqrt{r}}Y_1(\theta,\varphi)$ will produce a secular response. Therefore, its coefficient must vanish. This leads to the determination of A_1 which, so far, has been unknown:

$$A_1=7.8\quad. \tag{86}$$

Proceeding as before, we get a solution to the third-order equations:

$$u_3=A_3\frac{J_{3/2}(\alpha_1 r)}{r^{3/2}}P_1(\theta)-0.75\frac{J_{3/2}(\alpha_1 r)}{r^{3/2}}P_1(\theta)+2.0A_2\frac{J_{5/2}(\beta_1 r)}{r^{3/2}}P_2(\theta)+48\frac{J_{7/2}(\gamma_1 r)}{r^{3/2}}P_3(\theta)+\cdots$$

$$\tau_3=\frac{2A_3}{\alpha_1^3}\frac{J_{3/2}(\alpha_1 r)}{r^{1/2}}P_1(\theta)-0.11A_2\frac{J_{1/2}(\pi r)}{r^{1/2}}-0.063A_2\frac{J_{1/2}(2\pi r)}{r^{1/2}}$$

$$-\left\{0.74\frac{J_{3/2}(\alpha_1 r)}{r^{1/2}}+0.65\frac{J_{3/2}(\alpha_2 r)}{r^{1/2}}\right\}P_1(\theta)+0.18A_2\frac{J_{5/2}(\beta_1 r)}{r^{1/2}}P_2(\theta)$$

$$+\left\{4.8\frac{J_{7/2}(\gamma_1 r)}{r^{1/2}}+1.6\frac{J_{7/2}(\gamma_2 r)}{r^{1/2}}+0.53\frac{J_{7/2}(\gamma_3 r)}{r^{1/2}}+0.17\frac{J_{7/2}(\gamma_4 r)}{r^{1/2}}+\cdots\right\}P_3(\theta)+\cdots$$

$$v_3=A_3\left[\frac{J_{3/2}(\alpha_1 r)}{r^{3/2}}-\frac{\alpha_1}{2}\frac{J_{5/2}(\alpha_1 r)}{r^{1/2}}\right]\frac{\partial P_1(\theta)}{\partial\theta}-0.75\left[\frac{J_{3/2}(\alpha_2 r)}{r^{3/2}}+\frac{r}{2}\frac{d}{dr}\left(\frac{J_{3/2}(\alpha_2 r)}{r^{3/2}}\right)\right]\frac{\partial P_1(\theta)}{\partial\theta}$$

$$+1.0A_2r^2\left[\frac{J_{5/2}(\beta_1 r)}{r^{5/2}}+\frac{r}{3}\frac{d}{dr}\left(\frac{J_{5/2}(\beta_1 r)}{r^{5/2}}\right)\right]\frac{\partial P_2(\theta)}{\partial\theta}$$

$$+16r^3\left[\frac{J_{5/2}(\gamma_1 r)}{r^{7/2}}+\frac{r}{4}\frac{d}{dr}\left(\frac{J_{7/2}(\gamma_1 r)}{r^{7/2}}\right)\right]\frac{\partial P_3(\theta)}{\partial\theta}+\cdots,\qquad w_3=0 \tag{87}$$

where γ_i are the roots of $J_{7/2}$: $J_{7/2}(\gamma_i)=0$, $(i=1, 2\cdots)$.

§ 8. In case of a rotating sphere, calculations become more complicated, as another parameter Ω enters which is indicative of rotation. The physical quantities are expanded in double powers of ε and Ω. The followings are concerned only with the first order of ε and Ω. The chief result obtained is that the upwelling site on the surface is decided uniquely in relation to the rotating axis of the sphere.

In this case the equation of motion is, instead of (51),

$$0=-\operatorname{grad}\tilde{\omega}+\frac{C}{2}\vec{r\tau}+\nabla^2\vec{u}-\Omega\vec{e}\times\vec{u}, \tag{88}$$

where $\Omega=2\omega R^2/\nu$, ω is the angular velocity of rotation and $\vec{e}=(\cos\theta, -\sin\theta, 0)$ is the unit vector of rotation.

First of all, we expand C, u, and τ in the following form,

$$\left.\begin{aligned} C&=(1+\varepsilon^2)\sum_{n=0}^{\infty}C_n\Omega^n\\ \vec{u}&=\sum_{\substack{n=0\\ m=1}}^{\infty}\varepsilon^n\Omega^m\vec{u}_{n,m},\quad \vec{\tau}=\sum_{\substack{n=1\\ m=0}}^{\infty}\varepsilon^n\Omega^m\tau_{n,m}\end{aligned}\right\} \tag{89}$$

and then insert (89) into the governing equations (49), (50) and (88). The coefficients of $\varepsilon\Omega$ become as follows,

$$\operatorname{div}\vec{u}_{1,1}=0 \tag{90}$$

$$-2\vec{r}\vec{u}_{1,1}=\nabla^2\tau_{1,1} \tag{91}$$

$$\nabla^2\vec{u}_{1,1}-\operatorname{grad}\tilde{\omega}_{1,1}+\frac{C_0}{2}\vec{r}\left\{\tau_{1,1}+\frac{C_1}{C_0}\tau_{1,0}\right\}+\vec{u}_{1,0}\times\vec{e}=0, \tag{92}$$

where $\vec{u}_{1,0}$ and $\tau_{1,0}$ are respectively previous $\vec{u}_1$ and τ_1 of § 7.

From (90), (91) and (92),

$$\nabla^6(ru_{1,1})-C_0L^2(ru_{1,1})+\frac{C_1}{2}L^2\nabla^2\tau_{1,0}-\nabla^2\{\vec{r}\cdot\operatorname{rot}\operatorname{rot}(\vec{u}_{1,0}\times\vec{e})\}=0. \tag{93}$$

Hitherto, the direction of the motion $\vec{u}$ at the centre of the sphere has been undetermined. But in case of rotation, it must be decided in relation to the axis of rotation. Therefore $\vec{u}_{1,0}$ is not given by (73), (80) and (81) as before, but

$$\vec{u}_{1,0}\begin{pmatrix}u_{1,0}\\ v_{1,0}\\ w_{1,0}\end{pmatrix}=\begin{pmatrix}(F_{1,0}+r^2G_{1,0})rY_1(\theta\cdot\varphi)\\ F_{1,0}r\dfrac{\partial Y_1}{\partial\vartheta}\\ F_{1,0}r\dfrac{\partial Y}{\sin\theta\partial\varphi}\end{pmatrix} \tag{94}$$

where $Y_1=\bar{a}\cos\theta+\bar{b}\sin\theta\sin\varphi+\bar{c}\sin\theta\cos\varphi$ and $\bar{a}$, $\bar{b}$, and $\bar{c}$ are to be decided.

Inserting (94) into (93) we get

$$\nabla^6(ru_{1,1})-C_0L^2(ru_{1,1})-\nabla^2\left[\frac{J_{3/2}(\alpha_1r)}{\sqrt{r}}\left\{\frac{2C_1}{\alpha_1^2}\bar{a}\cos\theta+\bar{b}\sin\theta\sin\varphi+\bar{c}\sin\theta\cos\varphi\right)+\frac{\alpha_1^2}{2}(\bar{b}\sin\theta\cos\varphi-\bar{c}\sin\theta\sin\varphi)\right\}\Big]=0 \tag{95}$$

The inhomogeneous terms must vanish identically. Therefore,

$$C_1\bar{a}=0,\quad \frac{2C_1\bar{b}}{\alpha_1^2}-\frac{\alpha_1^2}{2}\bar{c}=0,\quad \frac{2C_1}{\alpha_1^2}\bar{c}+\frac{\alpha_1^2}{2}\bar{b}=0 \tag{96}$$

i.e.,

$$C_1=0,\ \bar{b}=0,\ \bar{c}=0. \tag{97}$$

This means that the fluid motion $\vec{u}_{1,0}$ is parallel to the axis of rotation at the centre of the sphere.

$\vec{u}_{1,1}$ and $\tau_{1,1}$ are

$$u_{1,1}=\frac{J_{3/2}(\alpha_1r)}{r^{3/2}}(\bar{a}_{1,1}\cos\theta+\bar{b}_{1,1}\sin\theta\sin\varphi+\bar{c}_{1,1}\sin\theta\cos\varphi)$$

$$\tau_{1,1}=\frac{2}{\alpha_1^2}\frac{J_{3/2}(\alpha_1r)}{r^{3/2}}(\bar{a}_{1,1}\cos\theta+\bar{b}_{1,1}\sin\theta\sin\varphi+\bar{c}_{1,1}\sin\theta\cos\varphi)$$

$$v_{1,1}=\left\{\frac{J_{3/2}(\alpha_1r)}{r^{3/2}}-\frac{\alpha_1}{2}\frac{J_{5/2}(\alpha_1r)}{r^{1/2}}\right\}(-\bar{a}_{1,1}\sin\theta+\bar{b}_{1,1}\cos\theta\sin\varphi+\bar{c}_{1,1}\cos\theta\cos\varphi)$$

$$w_{1,1}=\left\{\frac{J_{3/2}(\alpha_1r)}{r^{3/2}}-\frac{\alpha_1}{2}\frac{J_{5/2}(\alpha_1r)}{r^{1/2}}\right\}(\bar{b}_{1,1}\cos\varphi-\bar{c}_{1,1}\sin\varphi)-0.43\frac{J_{5/2}(\alpha_1r)}{r^{3/2}}\sin2\theta, \tag{98}$$

where $\bar{a}_{1,1}$, $\bar{b}_{1,1}$, and $\bar{c}_{1,1}$, are all unknowns which are determined in a later stage. The general pattern of motion $-\frac{J_{5/2}(\alpha_1r)}{r^{3/2}}\sin2\theta$ is shown in Fig. 8. It is already indicative of influence of the rotation.

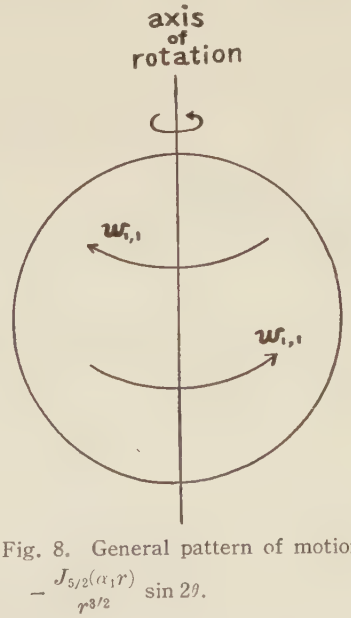

Fig. 8. General pattern of motion $-\frac{J_{5/2}(\alpha_1r)}{r^{3/2}}\sin2\vartheta$.

§ 9. In the remainder of this article, a study will be made of the steady thermal convection in a two-dimensional fluid layer when it is heated uniformly from below under a simultaneous constraint of non-uniform temperature on its upper surface (inhomogeneous boundary conditions). The fundamental equations are (9) and (10). The boundary conditions are also (11) except $\tau=0$, $(y=0)$.

As for the non-uniform temperature distribution on the upper surface, it is assumed to have a periodicity of wave length L, where $L=nl$, l is $2\sqrt{2}$, the wave length of spontaneous cells, and n is an integer. Under the assumption, it is expected that our model (Fig. 9) having a wave length L corresponds

Fig. 9. Geometry of the fluid layer under investigation.

to a spherical shell. In this study n is taken as 4. The non-uniformity is expressed as follows;

$$\left.\begin{aligned}&\tau_i=0, \qquad (i\neq 3)\\ &\tau_3=\sum_{n=1}^{\infty}\frac{8\sqrt{3}}{2\pi}\delta_n\cos\frac{2\pi}{8\sqrt{2}}n(x+\theta_n),\end{aligned}\right\}\ (y=1) \tag{99}$$

where δ_n's are arbitray.
As seen from (99), the non-uniformity is solely borne on τ_3 for the sake of mathematical technique.

§ 10. In this section, calculations are carried out as in § 3.

[ε]: The equations are

$$\begin{cases}\nabla^4\psi_1=R_0\dfrac{\partial\tau_1}{\partial x}\\ \dfrac{\partial\psi_1}{\partial x}=\nabla^2\tau_1.\end{cases} \tag{100}$$

The boundary conditions are

$$\frac{\partial\psi_1}{\partial x}=0,\quad \frac{\partial^2\psi_1}{\partial y^2}-\frac{\partial^2\psi_1}{\partial x^2}=0,\quad \tau_1=0,\ (y=0,\ 1). \tag{101}$$

The solution is

$$\begin{cases}\psi_1=A_1\sin\pi y\sin\dfrac{\pi}{\sqrt{2}}(x+x_1) & (102)\\ \tau_1=-\dfrac{\sqrt{2}\,A_1}{3\pi}\sin\pi y\cos\dfrac{\pi}{\sqrt{2}}(x+x_1). & (103)\end{cases}$$

It is to be noted here that besides A_1, an unknown phase, x_1, enters into ψ_1 and τ_1. This comes from the consideration that the site of spontaneous convection cells is to be decided according to the surface temperature disturbance. In fact, x_1 is determined later.

[ε^2]: The equations are

$$\begin{cases}\nabla^4\psi_2=R_0\dfrac{\partial\tau_2}{\partial x} & (104)\\ \dfrac{\partial\psi_1}{\partial y}\dfrac{\partial\tau_1}{\partial x}-\dfrac{\partial\psi_1}{\partial x}\dfrac{\partial\tau_1}{\partial y}+\dfrac{\partial\psi_2}{\partial x}=\nabla^2\tau_2. & (105)\end{cases}$$

The boundary conditions are

$$\frac{\partial\psi_2}{\partial x}=0,\quad \frac{\partial^2\psi_2}{\partial y^2}-\frac{\partial^2\psi_2}{\partial x^2}=0,\quad \tau_2=0,\ (y=0,1).$$

The solution is

$$\begin{cases}\psi_2=A_2\sin\pi y\sin\dfrac{\pi}{\sqrt{2}}(x+x_2) & (106)\\ \tau_2=-\dfrac{\sqrt{2}\,A_2}{3\pi}\sin\pi y\cos\dfrac{\pi}{\sqrt{2}}(x+x_2)\\ \qquad -\dfrac{A_1^2}{24\pi}\sin 2\pi y. & (107)\end{cases}$$

In this stage too, a new unknown phase x_2 appears.

[ε^3]:

$$\begin{cases}\nabla^4\psi_3=R_0\dfrac{\partial\tau_3}{\partial x}+R_0\dfrac{\partial\tau_1}{\partial x} & (108)\\ \dfrac{\partial\psi_1}{\partial y}\dfrac{\partial\tau_2}{\partial x}+\dfrac{\partial\psi_2}{\partial y}\dfrac{\partial\tau_1}{\partial x}-\dfrac{\partial\psi_1}{\partial x}\dfrac{\partial\tau_2}{\partial y}\\ \qquad -\dfrac{\partial\psi_2}{\partial x}\dfrac{\partial\tau_1}{\partial y}+\dfrac{\partial\psi_3}{\partial x}=\nabla^2\tau_3. & (109)\end{cases}$$

The boundary conditions are from (99) and (11)

$$\frac{\partial\psi_3}{\partial x}=0,\quad \frac{\partial^2\psi_3}{\partial y^2}-\frac{\partial^2\psi_3}{\partial x^2}=0,\quad (y=0,1),$$
$$\tau_3=0,\quad (y=0) \tag{110}$$
$$\tau_3=\frac{8\sqrt{2}}{2\pi}\sum_{n=1}^{\infty}\delta_n\cos\frac{2\pi}{8\sqrt{2}}n(x+\theta_n),\quad (y=1). \tag{111}$$

In the first place, (108) and (109) are cross-differentiated and then subtracted in order to get an equation governing ψ_3.

$$\nabla^6\psi_3-\frac{27}{4}\pi^4\frac{\partial^2\psi_3}{\partial x^2}$$
$$=\frac{\pi^2}{2}A_1R_0\left[\frac{A_1^2}{24}-1\right]\sin\pi y\sin\frac{\pi}{\sqrt{2}}(x+x_1)$$
$$-1352A_1^3\sin 3\pi y\sin\frac{\pi}{\sqrt{2}}(x+x_1). \qquad (112)$$

Considering (111) we seek a solution of the form

$$\psi_3=\sum_{n=1}^{\infty}f_n(y)\sin\frac{2\pi}{8\sqrt{2}}n(x+\theta_n)$$
$$+0.000164A_1^3\sin\pi y\sin\frac{\pi}{\sqrt{2}}(x+x_1), \qquad (113)$$

where the last term in (113) is the particular integral of $-1352A_1^3\sin\pi y\sin\frac{\pi}{\sqrt{2}}(x+x_1)$ of (112).

As the following manipulation is somewhat complicated, it will help us to rewrite the boundary conditions using f_n's:

$$f_n=0,\quad \ddot{f}_n=0 \qquad (y=0,\ 1) \qquad (114)$$
$$\dddot{f}_n=0, \qquad (y=0) \qquad (115)$$
$$\dddot{f}_n=-R_0n\delta_n \qquad (y=1) \qquad (116)$$

Now the problem is concerned with the functions f_n's. Of all these f_n's, f_4 is the most difficult one to deal with.

i) f_4. From (112) and (113) it is seen that

$$x_1=\theta_4 \qquad (117)$$

i.e., the phase, x_1, has been determined.

The equation governing f_4 is

$$\left[\frac{d^2}{dy^2}-\frac{\pi^2}{2}\right]^3f_4(y)+\left(\frac{3\pi^2}{2}\right)^3f_4(y)$$
$$=\frac{A_1R_0}{2}\pi^2\left[\frac{A_1^2}{24}-1\right]\sin\pi y\,. \qquad (118)$$

The general solution $f_4(y)$ of (118) is the sum of the homogeneous solution $\sum_{i=1}^{6}a_ih_i(y)$ plus a particular integral $\bar{f}_4(y)$;

$$\bar{f}_4(y)=-\frac{3.70A_1R_0}{10^2\pi^3}\left[\frac{A_1^2}{24}-1\right]y\cos\pi y, \qquad (119)$$

i.e.,
$$f_4(y)=\sum_{n=1}^{5}a_ih_i(y)$$
$$-\frac{3.70A_1R_0}{10^2\pi^3}\left[\frac{A_1^2}{24}-1\right]y\cos\pi y, \qquad (120)$$

where a_i's have not been determined as yet, and $h_i(y)$'s are the solution to the homogeneous equation of (118);

$$\left[\frac{d^2}{dy^2}-\frac{\pi^2}{2}\right]^3h_i(y)+\left(\frac{3\pi^2}{2}\right)^3h_i(y)=0, \qquad (121)$$

$$(h_1,\cdots h_6)=(\sin\pi y,\ \cos\pi y,\ e^{(3,94+1,62i)y},$$
$$e^{-(3,94+1,62i)y},\ e^{(3,94-1,62i)y},\ e^{-(3,94-1,62i)y}). \qquad (122)$$

Next we have to make (120) satisfy the boundary conditions (114), (115) and (116):

$$\left.\begin{aligned}
&\sum_{i=2}^{6}a_ih_i(0)=0,\\
&\sum_{i=2}^{6}a_ih_i(1)=\frac{-3.70A_1R_0}{10^2\pi^3}\left[\frac{A_1^2}{24}-1\right],\\
&\sum_{i=2}^{6}a_i\ddot{h}_i(0)=0,\\
&\sum_{i=2}^{6}a_i\ddot{h}_i(1)=\frac{3.70A_1R_0}{10^2\pi}\left[\frac{A_1^2}{24}-1\right],\\
&\sum_{i=2}^{6}a_i\dddot{h}_i(0)=0,\\
&\sum_{i=2}^{6}a_i\dddot{h}_i(1)=\frac{-3.70A_1R_0\pi}{10^2}\left[\frac{A_1^2}{24}-1\right]\\
&\qquad -4R_0\delta_4\,,
\end{aligned}\right\} \qquad (123)$$

where the summation on the left-hand side is, as noted above, from 2 to 6. This is because $h_1=\sin\pi y$ vanishes on the boundaries and need not be written down. In (123) there are six linear equations while the number of unknowns a_i's are only five. Therefore if (123) is to be consistent, all of the equations cannot be linearly independent. There must be six of such ξ_i's as, when multiplied by the equations (123) respectively in order, and summed up, will make the coefficients of a_i's vanish:

$$\xi_1h_i(0)+\xi_2h_i(1)+\xi_3\ddot{h}_i(0)+\xi_4\ddot{h}_i(1)+\xi_5\dddot{h}_i(0)$$
$$+\xi_6\dddot{h}_i(1)=0, \quad (i=2\cdots6). \qquad (124)$$

From (124), ξ_i's are determined

$$\xi_2=1,\ \xi_3=\frac{10}{13\pi^2},\ \xi_4=-\frac{10}{13\pi^2},\ \xi_5=\frac{4}{13\pi^4}$$
$$\xi_6=\frac{4}{13\pi^4}, \qquad (125)$$

where ξ_1 is taken as 1.

One more thing must be added. If (123) is consistent at all, these ξ_i's must also satisfy the following relation:

$$3.70A_1R_0\left[\frac{A_1^2}{24}-1\right](-\xi_2+\pi^2\xi_4-\pi^4\xi_6)$$
$$-4R_0\delta_4\xi_6=0 \qquad (126)$$

which is derived from the inner product of the right-hand side of (123) and ξ_i's. (126) contains A_1 so far unknown. This means that (126) is the equation determining A_1. Inserting (125) into (126), the final relation determining A_1 is obtained:

$$A_1\left[\frac{A_1^2}{24}-1\right]=\frac{-16}{\pi}\delta_4. \qquad (127)$$

The relation (127) is represented in Fig. 10. In some cases, for a given δ_4 there may be three A_1's which formally satisfy (127), e.g., A_1, A_1' and A_1'' in Fig. 10. Of these three

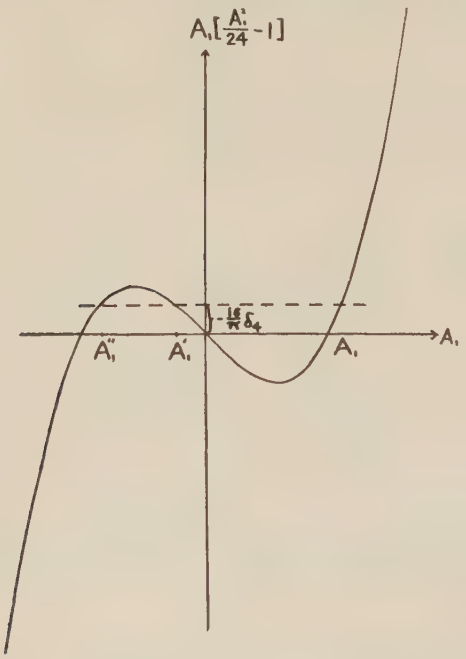

Fig. 10. Curve for deciding the amplitude of a spontaneous cell.

A_1's, only A_1 is the one we want, for with continuous increase of δ_4, A_1' and A_1'' suddenly cease to exist. This means that A_1' and A_1'' have no physical counterparts.

The procedure to get to the relation (127) was somewhat circuitous. In another simple way, (127) is also obtainable. As in case of the GREEN's integral theorem, we first consider the homogeneous equation of (118);

$$\mathscr{L}[\sin\pi y]\equiv\left[\frac{d^2}{dy^2}-\frac{\pi^2}{2}\right]^3\sin\pi y$$
$$+\left(\frac{3\pi^2}{2}\right)^3\sin\pi y=0 \qquad (128)$$

with a solution, $\sin\pi y$ put into it. Then multiplying (128) by $f_4(y)$ and (118) by $\sin\pi y$ respectively, integrating them both from 0 to 1, and finally subtracting one from the other, we get

$$\int_0^1\{f_4\,\mathscr{L}[\sin\pi y]-\sin\pi y\,\mathscr{L}[f_4]\}dy$$
$$=-\frac{A_1R_0}{4}\pi^2\left[\frac{A_1^2}{24}-1\right]. \qquad (129)$$

This is the same as (127), as easily seen on integrating the left-hand side of (129) by parts. Although the present method is easier, we cannot fully rely on it, for from (129) the functional form of $f_4(y)$ cannot be obtained.

ii) f_n $(n\neq 4)$. The governing equation is

$$\nabla^6 f_n(y)\sin\frac{2}{8\sqrt{2}}n(x+\theta_n)$$
$$-\frac{27}{4}\pi^4 f_n(y)\frac{d^2}{dx^2}\sin\frac{2\pi}{8\sqrt{2}}n(x+\theta_n)=0. \qquad (130)$$

The boundary conditions are

$$f_n(y)=0,\ \ddot{f}_n(y)=0,\ (y=0,1),\ \ddddot{f}_n(y)=0,\ (y=0), \qquad (131)$$

$$\ddddot{f}_n(y)=-nR_0\delta_n,\ (y=1). \qquad (132)$$

We seek a solution in the form

$$f_n(y)=\sum_{i=1}^{3}c_i^{\pm}e^{\pm p_i y}, \qquad (133)$$

where $c_i^{\pm}$'s are unknown constants and p_i's are the roots of

$$\left(p^2-\frac{n^2\pi^2}{32}\right)^3+\frac{27\pi^3}{128}n^2=0 \qquad (134)$$

i.e.,

$$p_1^2=\frac{n^2\pi^2}{32}-\frac{3\pi^2}{4}\left(\frac{n^2}{2}\right)^{1/3}\equiv-s^2,\ p_2^2=\frac{n^2\pi^2}{32}$$
$$+\frac{3\pi^2}{8}\left(\frac{n^2}{2}\right)^{1/3}(1+\sqrt{3}\,i)\equiv(q+ri)^2,\ p_3^2=(q-ri)^2. \qquad (135)$$

Taking the boundary conditions (131) and (132) into account, we get for f_n

$$f_n=\frac{nR_0\delta_n}{qr\{(s^2+q^2+r^2)^2-4q^2r^2\}}\Big[-qr\frac{\sin sy}{\sin s}$$
$$+\frac{s^2+q^2-r^2}{\sqrt{3}\,(e^{2q}+e^{-2q}-2\cos 2r}\Big\{e^{q(y+1)}\cos\Big(r\bar{y}-1+\frac{\pi}{3}\Big)$$
$$+e^{-q(y+1)}\cos\Big(r\overline{y-1}-\frac{\pi}{3}\Big)-e^{q(y-1)}\cos\Big(r\overline{y+1}+\frac{\pi}{3}\Big)$$
$$-e^{-q(y-1)}\cos\Big(r\overline{y+1}-\frac{\pi}{3}\Big)\Big\}\Big] \qquad (n\neq 4). \qquad (136)$$

To sum up, ψ_3 becomes as follows;

$$\psi_3=A_3\sin\pi y\sin\frac{\pi}{\sqrt{2}}(x+x_3)$$
$$+0.000164A_1^3\sin 3\pi y\sin\frac{\pi}{\sqrt{2}}(x+\theta_4)$$
$$+\sum_{n=1}^{\infty}\delta_n f_n(y)\sin\frac{2\pi}{8\sqrt{2}}n(x+\theta_n)\,, \qquad (137)$$

where f_n's are shown in Fig. 11. Of these f_n's, f_3 and f_5 are larger in value than other

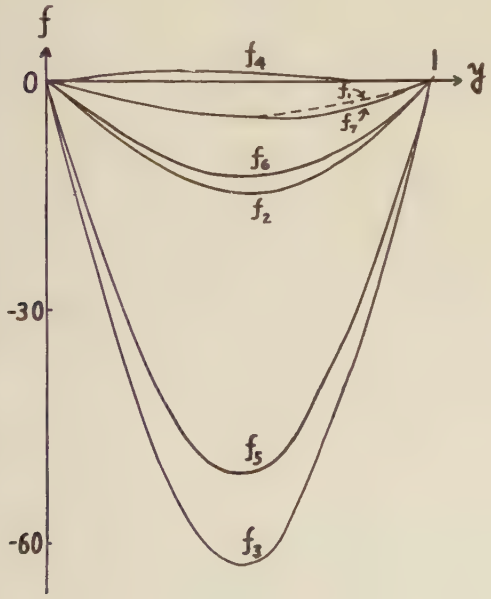

Fig. 11. f_i's in (48).

f_n's. This is due to the fact that, in case of f_3, and f_5, $\sin s$ in (136) is nearly zero.

τ_4 is obtained from the auxiliary equation (108) or (109).

$$\tau_3=-\frac{A_1A_2}{12\pi}\cos\frac{\pi}{\sqrt{2}}(\theta_4-x_2)\sin 2\pi y$$
$$-\frac{\sqrt{2}\,A_3}{3\pi}\sin\pi y\cos\frac{\pi}{\sqrt{2}}(x+x_3)$$
$$-0.000986A_1^3\sin 3\pi y\cos\frac{\pi}{\sqrt{2}}(x+\theta_4)$$
$$+0.00623A_1^3\sin\pi y\cos\frac{\pi}{\sqrt{2}}(x+\theta_4)$$
$$+\sum_{n=1}^{\infty}\delta_n g_n(y)\cos\frac{2\pi}{8\sqrt{2}}n(x+\theta_n), \qquad (138)$$

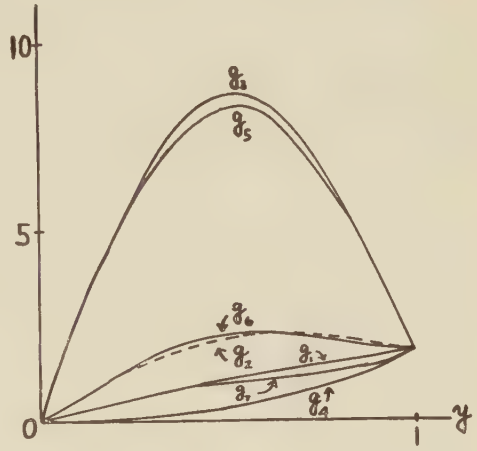

Fig. 12. f_i's in (50).

where g_n's are shown in Fig. 12. Among these, g_3 and g_5 are large by far.

[ε^4]: The equations are

$$\nabla^4\psi_4=R_0\frac{\partial\tau_4}{\partial x}+R_0\frac{\partial\tau_2}{\partial x}\,, \qquad (139)$$

$$\frac{\partial\psi_1}{\partial y}\frac{\partial\tau_3}{\partial x}+\frac{\partial\psi_2}{\partial y}\frac{\partial\tau_2}{\partial x}+\frac{\partial\psi_3}{\partial y}\frac{\partial\tau_1}{\partial x}-\frac{\partial\psi_1}{\partial x}\frac{\partial\tau_3}{\partial y}$$
$$-\frac{\partial\psi_2}{\partial x}\frac{\partial\tau_2}{\partial y}-\frac{\partial\psi_3}{\partial x}\frac{\partial\tau_1}{\partial y}+\frac{\partial\psi_4}{\partial x}=\nabla^2\tau_4. \qquad (140)$$

The boundary conditions are homogeneous. From (139) and (140) we get an equation governing ψ_4 and then the relation determining A_2:

$$\frac{A_2\pi^2}{2}\Big[\frac{A_1^2}{2}-1\Big]=0. \quad \therefore\ A_2=0. \qquad (141)$$

As to the convergency, it is seen that the terms of [ε^4] are negligible so long as $A_1\simeq 8$ and $\varepsilon^2\leq 1$. But the range of ε is narrowed still more in the stage of [ε^5], as inhomogeneous terms containing δ_3 and δ_5 produce a particular integral of a large value. Therefore in dealing with the δ_3 and δ_5 disturbances, enough consideration must be paid.

§ 11. It is of interest to see how the patterns of convection are changed by the inhomogeneity constrained on the surface. This will be seen from the following several examples.

i) The temperature difference between the upper and lower surfaces is 10% in excess of the critical value. The surface temperature disturbance is in the form $\cos\frac{\pi}{\sqrt{2}}x$ and its amplitude is 10% of the temperature difference ($\delta_4=1.75$). From (127), $A=-7.35$. Isothermals and stream lines in this case are shown in Fig. 13. The site of spontaneous cells is decided entirely according to the inhomogeneity on the surface. The upwelling site is where the upper surface temperature is the highest and the sinking site is where it is the lowest. But, the pattern itself is almost the same as that with no inhomogeneity on the surface. It is to be noted here that the inhomogeneous temperature disturbance having the critical wave length, $2\sqrt{2}$ in this case, decides once and for all the site of spontaneous convection cells, however small the disturbance may be.

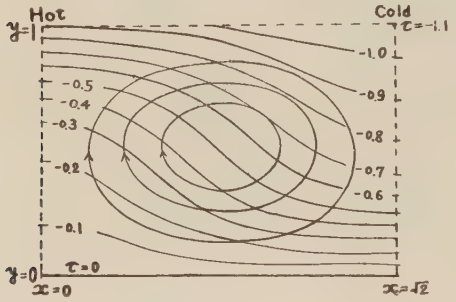

Fig. 13. Isothermals and stream lines when the temperature difference between the upper and lower surfaces is 10% in excess of the critical value. The surface temperature disturbance is of a form $\cos\frac{\pi}{\sqrt{2}}x$ and its amplitude is 10% of the temperature difference.

ii) The temperature difference between the upper and the lower surfaces is 10% in excess of the critical value. The surface temperature disturbance is

$$0.1T_{diff}\left[\cos\frac{\pi}{4\sqrt{2}}x+\frac{1}{2}\cos\frac{\pi}{\sqrt{2}}x\right].$$

Isothermals and stream lines in this case are shown in Fig. 14. It is seen from Fig. 14 that surface disturbances having much larger wave length than the critical one play very little part. Neither high nor low temperature sites on the surface seem to have considerable influence on a convective pattern. Much less can it be said from Fig. 14 that convective currents are upward where the temperature is low on the upper surface and downward where it is high. From this fact upward con-

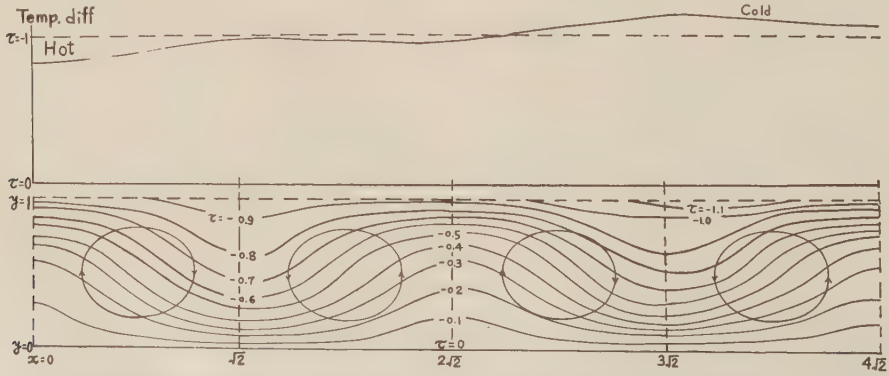

Fig. 14. Isothermals and stream lines when the temperature difference between the upper and lower surfaces is 10% in excess of the critical value. The surface temperature disturbance is $0.1\,T_{diff}\left[\cos\frac{\pi}{4\sqrt{2}}x+\frac{1}{2}\cos\frac{\pi}{\sqrt{2}}x\right]$, in other words, the amplitude for the wave length $8\sqrt{2}$ is 10% of the temperature difference, while that for the wave length $2\sqrt{2}$ is half as large.

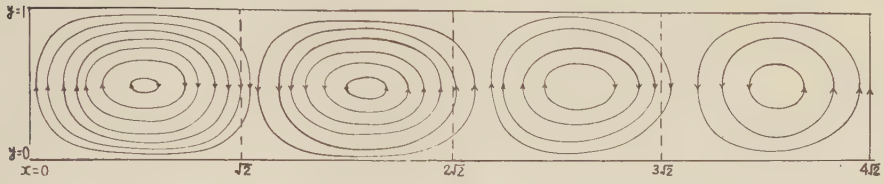

Fig. 15. Stream lines when the temperature difference between the upper and lower surfaces is only 0.3% in excess of the critical value. The surface temperature disturbance is $0.003\,T_{\text{diff}} \cos \frac{3\pi}{4\sqrt{2}} x + o(1) \cos \frac{\pi}{\sqrt{2}} x$, in other words, the amplitude for the wave length $\frac{8\sqrt{2}}{3}$ is 0.3% of the temperature difference, while that for the wave length $2\sqrt{2}$ is infinitesimal.

vective currents may not always be expected under the oceans where the temperature is comparatively low compared with under the continents.

iii) Surface disturbances having wave lengths close to the critical one have much influence in determining the general feature of fluid motion. In § 10, these are terms concerned with δ_3 and δ_5.

Shown in Fig. 15 are stream lines when the temperature difference between the lower and upper surfaces is only 0.3% in excess of the critical value and the surface temperature disturbance is

$$0.003\, T_{diff} \cos \frac{3\pi}{4\sqrt{2}} x + o(1) \cos \frac{\pi}{\sqrt{2}} x.$$

In this case, as the surface disturbance is very small, its influence is not seen very clearly. But if we compare Fig. 15 with Fig. 14, it is seen that the disturbance of δ_3 is very influential.

Fig. 16 shows the root mean square amplitude (in km) of a spherical harmonic of order l in the topographic analysis of the earth's surface after Vening Meinesz (1951). Chandrasekhar (1953) showed that the convective patterns of harmonics of orders three and four set in first when the depth of spherical shell is about half the radius of the sphere. Then he indicated the bearing of this result on the problem of convection in the earth's mantle and of the interpretation of the earth's topographic features. In this present article, it was shown that surface disturbances having much larger or smaller wave lengths than the critical one play very little part in determining the general feature of fluid motion, while those having wave lengths next to the

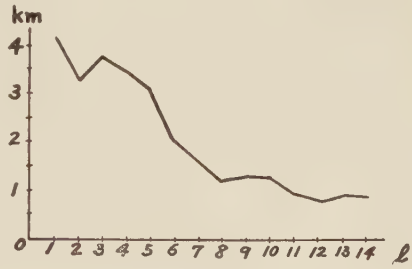

Fig. 16. Root mean square amplitude (in km) of a spherical harmonic of order l in the topographic analysis of the earth's surface after Vening Meinesz.

critical one are quite effective in this. This conclusion is of some interest as it is seen from Fig. 16 that the amplitude of a spherical harmonic of order 5 is considerably large compared with that of order 6.

In conclusion, the writer wishes to express his sincere thanks to Prof. C. Tsuboi and Dr. H. Takeuchi of Tokyo University for their encouragement and support throughout the course of this study. His thanks are also due to Prof. S. Chandrasekhar of Chicago University for calling his attention to Malkus and Veronis' study.

References

BIRCH, F:
1951 "Remarkes on the structure of the mantle and its bearing upon the possibility of convection currents". Trans. Amer. Geophys. Union, **32**, 533.

BLACKEETT, P.M.S.:
1956 "Lectures on rock magnetism". Jerusalem, Weitzmann Science Press.

BULLARD, E.C.:
1950 "The transfer of heat from the core of the earth". M.N.R.A.S.G.S., **6**, 36.

BULLARD, E.C.:
1954 "The earth as a planet". (Kuiper, G.P., ed.) Chapter 2. Chicago, Illinois.

BULLARD, E.C.:
1956 "Advances in geophysics". Volume 3. New York.

CHANDRASEKHAR, S.:
1952 "The thermal instability of a fluid sphere heated within". Phil. Mag. [7], **43**, 1317.

CHANDRASEKHAR, S.:
1953 "The onset of convection by thermal instability in spherical shells". Phil. Mag. [7], **44**, 233.

HALES, A. L.:
1936 "Convection currents in the earth". M.N.R.A.S.G.S., **3**, 372.

HASKELL, N.A.:
1936 "The motion of a viscous fluid under a surface load". Physics, **7**, 56.

MALKUS, W.V.R., and VERONIS, G.:
1958 "Finite amplitude cellular convection". J. Fluid Mech., **4**, 225.

RAYLEIGH, LORD:
1916 "On convection currents in a horizontal layer of fluid, when the higher temperature is on the under side". Phil. Mag., [6], **32**, 529.

VENING MEINESZ, F.A.:
1951 "A remarkable feature of the earth's topography, origin of continents and oceans". Proc. Kon. Ned. Akad. Wetensch., Series B, **54**, 212, 220.

Von HERZEN, R.:
1959 "Heat flow values from the South-Eastern Pacific". Nature, **183**, 882.

[Journal of the Faculty of Science, Hokkaidô University, Japan, Ser. VII, Vol. I, No. 3, 1959]

LOVE-waves in Stratified Three Layers

(Continued)

Hiroshi OKADA and Kyozi TAZIME

(Received Octover 22, 1959)

Abstract

At first, some examples are calculated of the dispersion curve, the amplitude function and the amplitude distribution for the first order of LOVE-waves. These calculations remained for cases (A) and (B) in eq. (57) in the previous paper[6].

Next, for cases (C) and (D) in eq. (57), the other examples for the zeroth and the first orders of LOVE-waves are presented.

Lastly, some physical considerations as to these calculations are given.

13. Numerical calculations of the dispersion curve for L_1 in cases (A) and (B)

The dispersion curve for the zeroth order of LOVE-waves, noted by L_0, were already calculated for cases (A) and (B) of (57) in Sec. 9. The rigidity ratios adopted in the numerical calculation were (a) $\mu_2/\mu_1=4$ and $\mu_3/\mu_2=30$, (b) $\mu_2/\mu_1=30$ and $\mu_3/\mu_2=30$, (c) $\mu_2/\mu_1=1/16$ and $\mu_3/\mu_2=30$ and (d) $\mu_2/\mu_1=1/3$ and $\mu_3/\mu_2=30$.

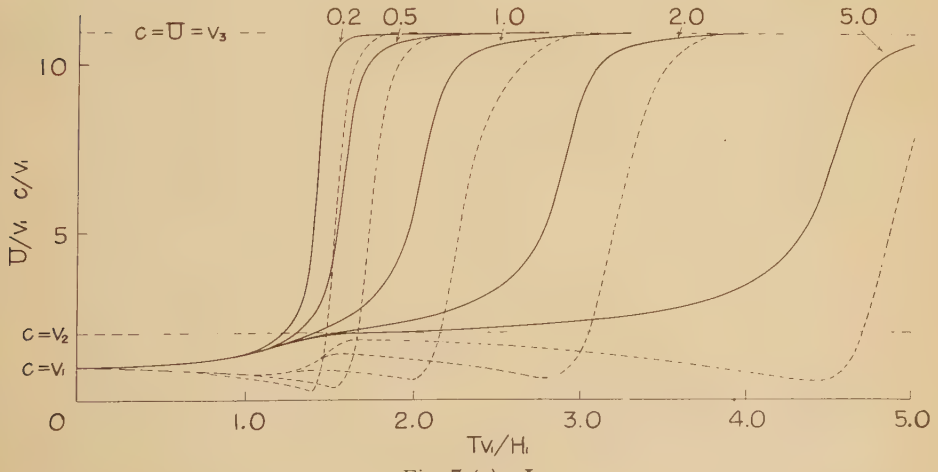

Fig. 7 (a). L_1

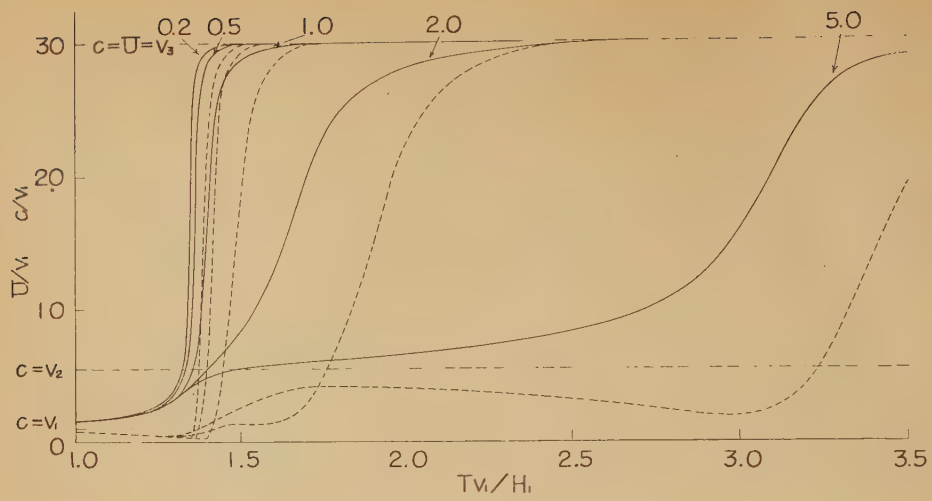

Fig. 7 (b). $\mathbf{L}_1$

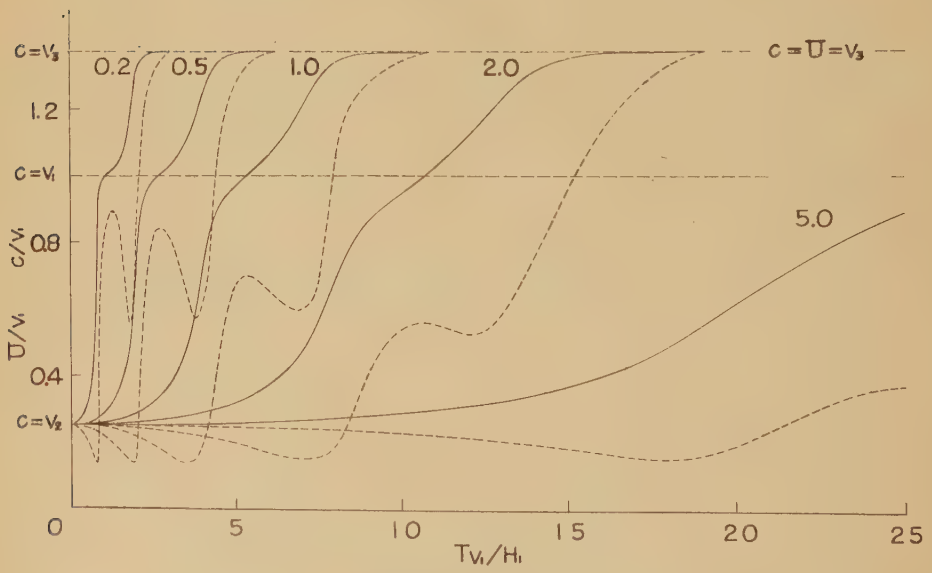

Fig. 7 (c). $\mathbf{L}_1$

The dispersion curve for the first order of Love-waves, noted by $\mathbf{L}_1$, has been calculated in this section, adopting the same rigidity ratios as before. The results are shown in Figs. 7(a) to 7(d) for various values of the parameter

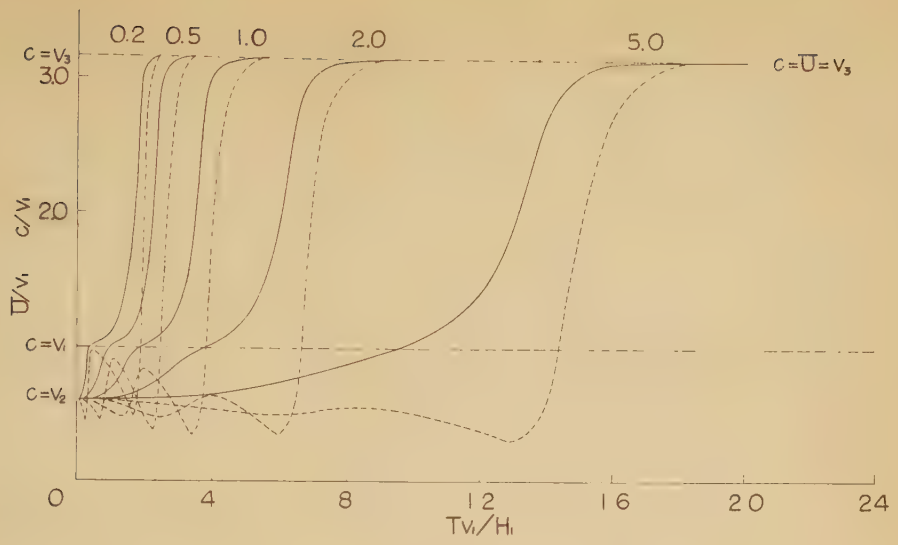

Fig. 7 (d). $\mathbf{L}_1$

Fig. 7. Dispersion curves for $\mathbf{L}_1$ in cases (A) and (B).
(a) $\mu_2/\mu_1 = 4$ and $\mu_3/\mu_2 = 30$, (b) $\mu_2/\mu_1 = 30$ and $\mu_3/\mu_2 = 30$
(c) $\mu_2/\mu_1 = 1/16$ and $\mu_3/\mu_2 = 30$, (d) $\mu_2/\mu_1 = 1/3$ and $\mu_3/\mu_2 = 30$

H_2/H_1.

Whereas $\mathbf{L}_0$ has no cutoff period, $\mathbf{L}_1$ has a finite cutoff period at which phase- and group-velocities must coincide with the velocity of S-wave in the lowest layer. Periods of $\mathbf{L}_1$ must be confined between the cutoff and zero.

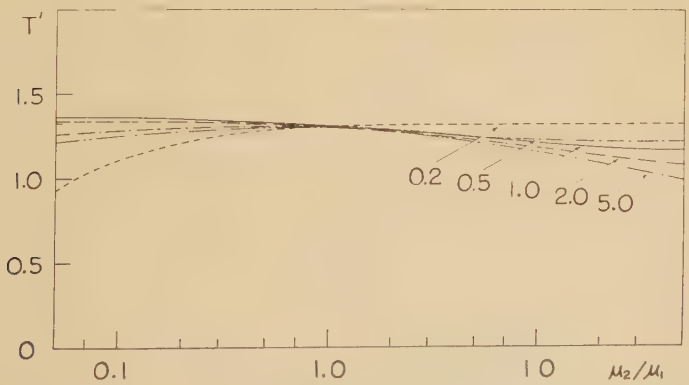

Fig. 8. The period corresponding to the second minimum group velocity for $\mathbf{L}_1$ in cases (A) and (B). $T' = T/(H_1/v_1 + H_2/v_2)$.

Group velocity has two minima as in the case of the zeroth order; one is near $T/(H_1/v_1) = 4/3$ and another is near $T/(H_1/v_1+H_2/v_2)=4/3$, for the rigidity ratios (a) and (b). The latter relation will be clear from Fig. 8 where μ_3/μ_2 is kept at 30.

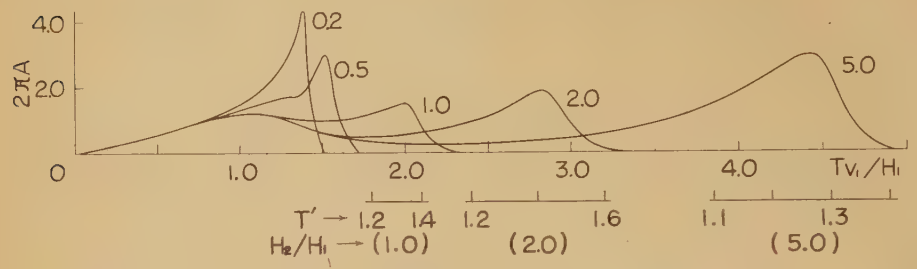

Fig. 9 (a). $\mathbf{L}_1$

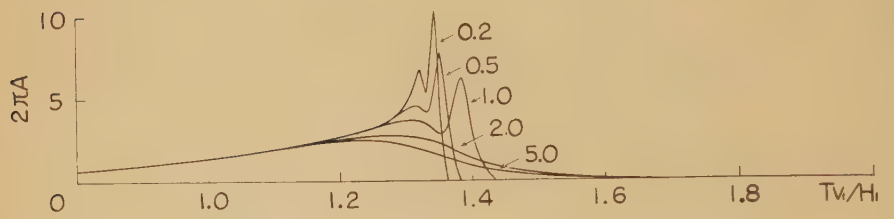

Fig. 9 (b). $\mathbf{L}_1$

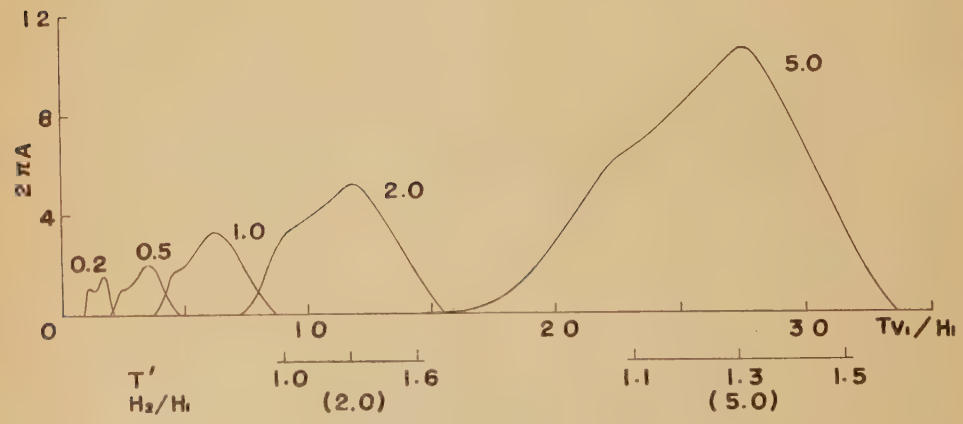

Fig. 9 (c). $\mathbf{L}_1$

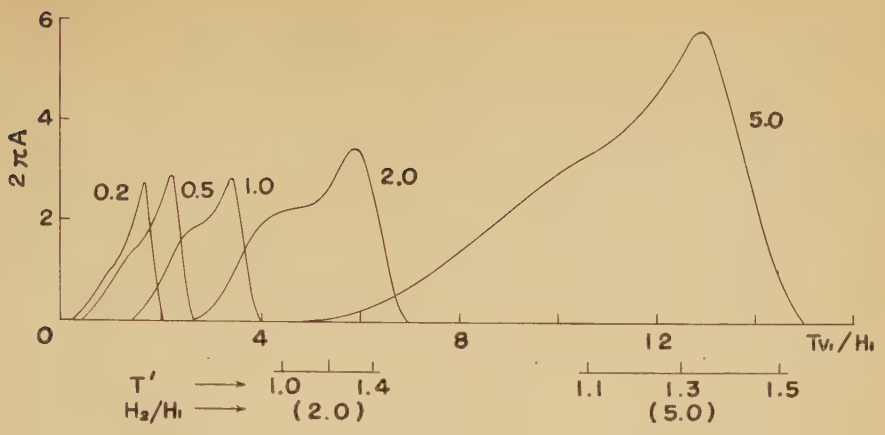

Fig. 9 (d). $\mathbf{L}_1$

Fig. 9. Amplitude functions for $\mathbf{L}_1$ in cases (A) and (B).
$T' = T/(H_1/v_1+H_2/v_2)$.

14. Numerical calculations of the amplitude fuuction for $\mathbf{L}_1$ in cases (A) and (B)

The amplitude function $2\pi A(\xi)$ in (45) has been obtained by using the dispersion curve illustrated in Fig. 7. The results are shown in Figs. 9 (a) to 9 (d) as functions of period Tv_1/H_1.

These amplitude functions may have two maxima in each case. It must be noticed that the first maximum in cases (c) and (d) occurs respectively near the period of the maximum group velocity, whereas the other maxima,

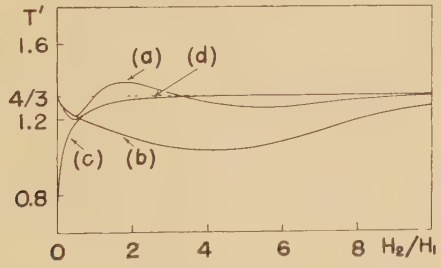

Fig. 10. The period corresponding to the second maximum of the amplitude function for $\mathbf{L}_1$ in cases (A) and (B).
$T'=T/(H_1/v_1+H_2/v_2)$.
(a) : (4, 30), (b) : (30, 30), (c) : (1/16, 30), (d) : (1/3, 30)

the first maximum in cases (a) and (b) and the second maximum in all cases, occur respectively near the period of the minimum group velocity.

Fig. 10 shows the relation between the period of the second maximum of the amplitude function and H_2/H_1, being parameters $(\mu_2/\mu_1,\ \mu_3/\mu_2)$. It is clear that each curve will approach to the period indicated by $T/(H_1/v_1+H_2/v_2)=4/3$ with the increase of H_2/H_1.

Now it has been found that either $\mathbf{L}_0$ or $\mathbf{L}_1$ must obey the wave-length law in general,

$$T/(H_1/v_1) \text{ or } T/(H_1/v_1+H_2/v_2)=4/(2n+1)\,,\quad \begin{pmatrix} n=0 \text{ for } \mathbf{L}_0 \\ =1 \text{ for } \mathbf{L}_1 \end{pmatrix} \qquad (64)$$

at least qualitatively. The thickness of the layers may have larger influence on $\mathbf{L}_1$ than on $\mathbf{L}_0$, because the former has shorter wave-length than the latter. Comparing Fig. 10 with Fig. 5, the asymptotic value of (64) seems to be easily attained by $\mathbf{L}_1$ rather than by $\mathbf{L}_0$. But the ratios of deviation from the asymptotic value are nearly equal to each other for the same value of H_2/H_1.

This situation may also be seen in the relation between the sharpness of the maximum of the amplitude function and the period. The higher the order of the waves, the narrower the band of the period having considerably large amplitude.

It will be physically expected that the amplitude function may arrive at the maximum near the period of the mimimum group velocity. Analytically, this phenomenon may be easily recognized by the factor $(v_1/U-v_1/c)$ in (45). On the other hand, it will seem strange that the amplitude function may arrive at the first maximum near the period of the maximum group velocity in cases (c) and (d). Numerically, the present authors have found that the factor $\{1-(v_1/c)^2\}^{-1}$ in (45) plays the greatest role in these cases.

The latter phenomenon must be accompanied by the "low velocity layer". Considerable energies will escape from the most superficial layer to the low velocity one. Thus the wave of short length cannot keep the law of (64), but ignores that law. Displacement of the wave of short length has the factor $\cosh \hat{\eta}_1 z$ as shown in (iii) of page 126. If c coincides with v_1, $\cosh \hat{\eta}_1 z$ becomes unity for each depth, resulting in large displacement on the surface of the earth for a certain amplitude on the lower boundary of the most superficial layer.

15. Numerical calculations of the amplitude distribution for $\mathbf{L}_1$ in cases (A) and (B)

Figs. 11(a) to 11(d) illustrate the results calculated for several periods

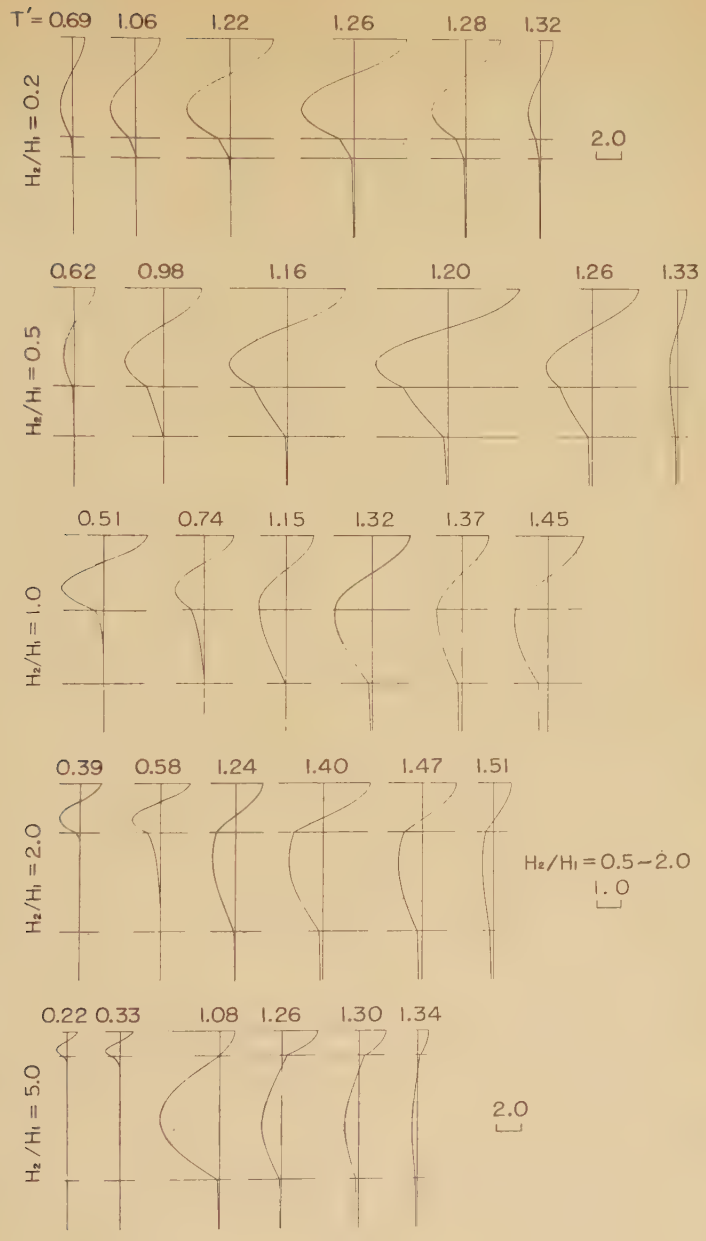

Fig. 11 (a). $\mathbf{L}_1$

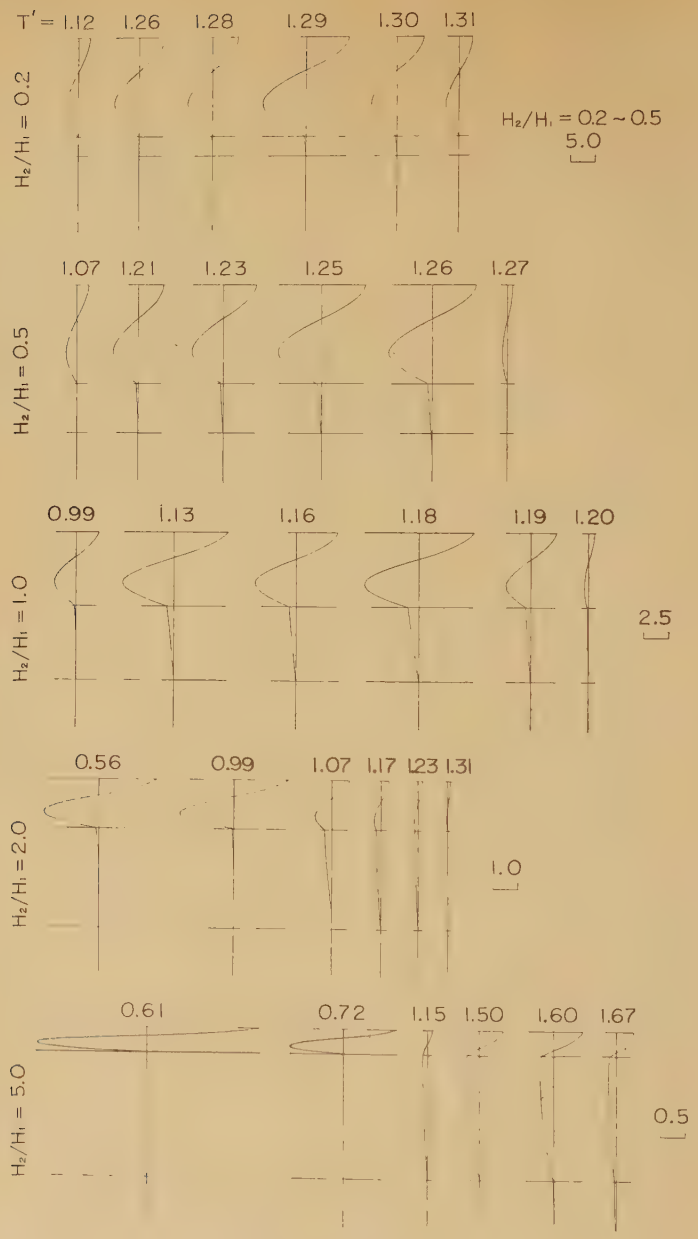

Fig 11 (b). $\mathbf{L}_1$

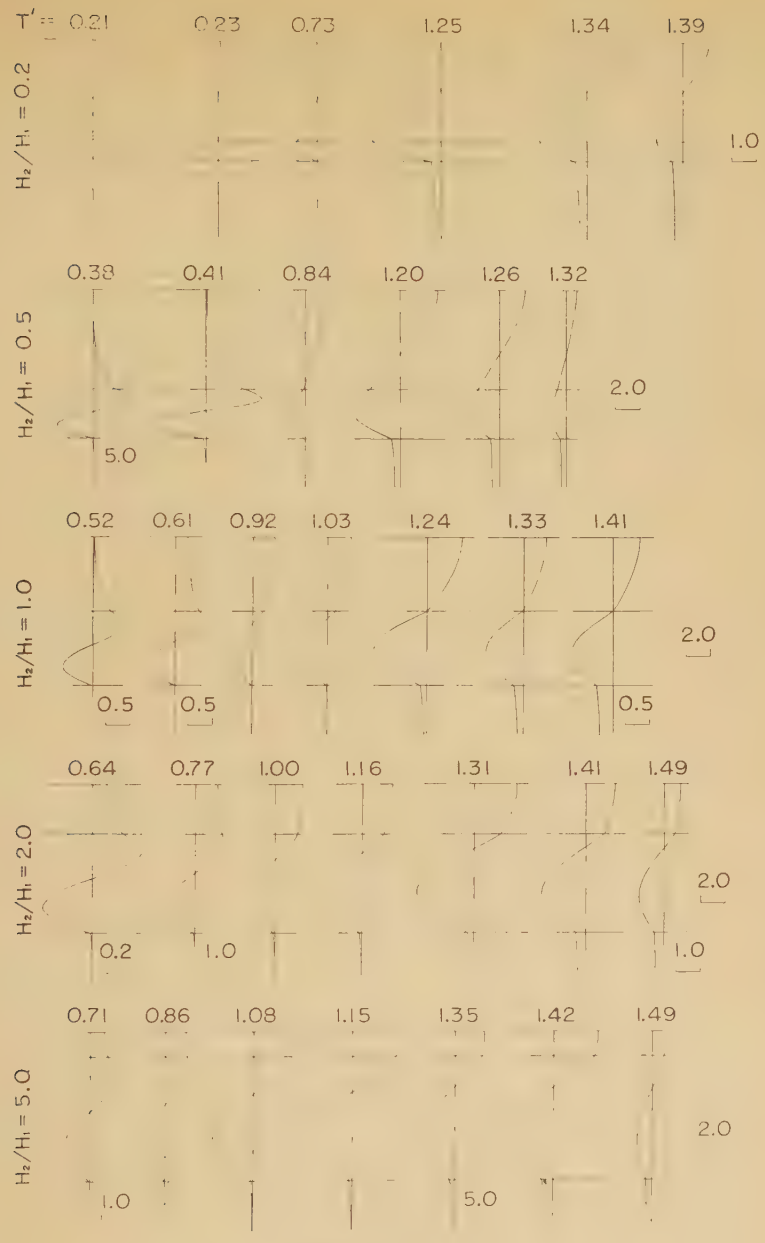

Fig. 11 (c). $\mathbf{L}_1$

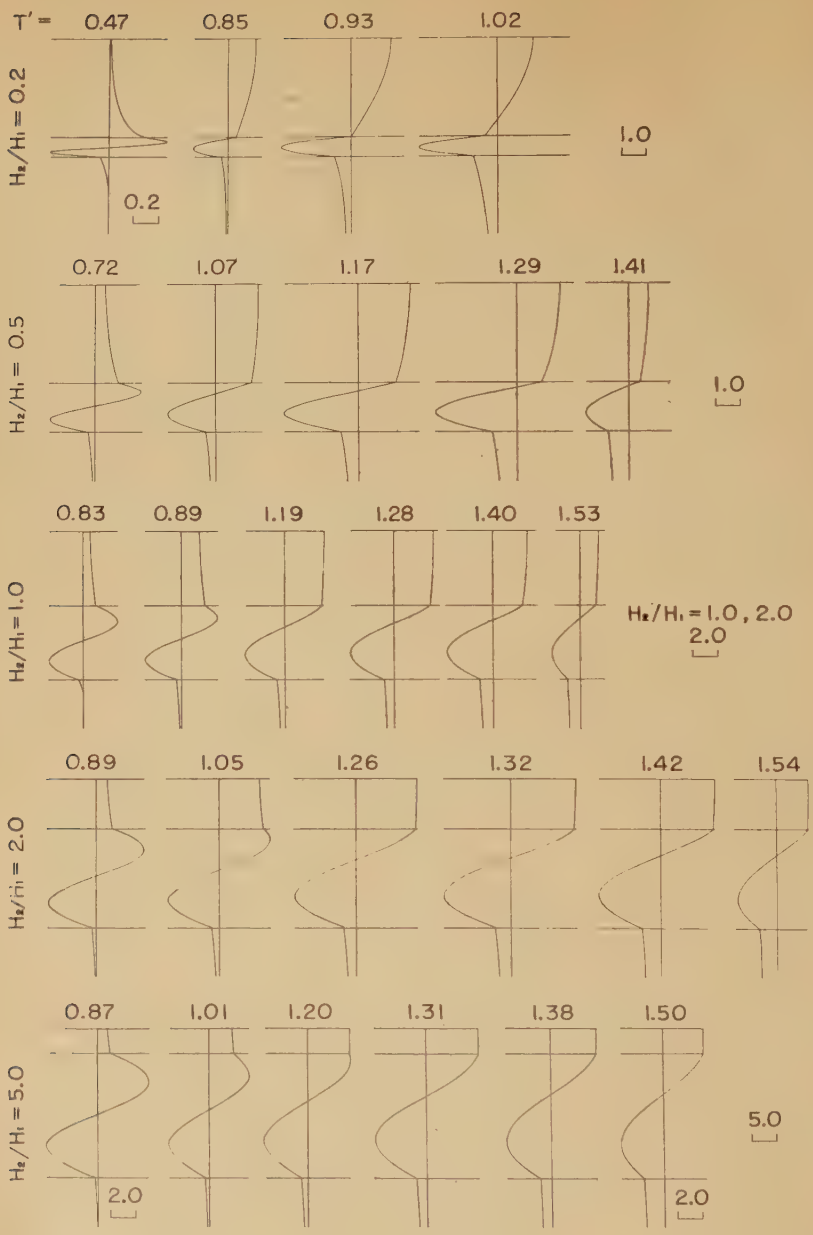

Fig. 11 (d) $\mathbf{L}_1$

Fig. 11. Amplitude distributions for $\mathbf{L}_1$ in cases (A) and (B).
$T' = T/(H_1/v_1 + H_2/v_2)$.

indicated by $T=T/(H_1/v_1+H_2/v_2)$.

Nodes are seen, in Figs. 11(a) and 11(b), in the most superficial layer for all periods. On the other hand in Figs. 11(c) and 11(d), the nodes migrate upwards in the low velocity layer and go into the upper layer with increasing periods.

Actual amplitude distribution does not always show handsome configuration forming 3/4 wave-lengths, whereas (64) is satisfied fairly well at the maximum of the amplitude function.

16. Numerical calculations of the dispersion curve for L_0 and L_1 in cases (C) and (D)

Case (C) from (57) may take the type (iii) in (26). The dispersion curve has been calculated by the characteristic equation (iii) in (27).

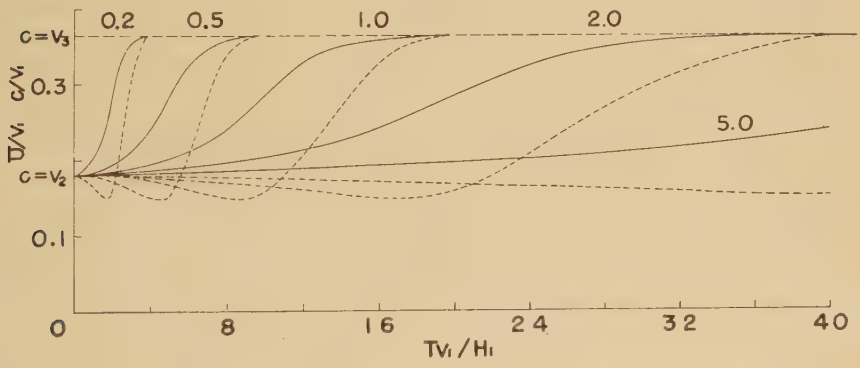

Fig. 12 (a). L_0

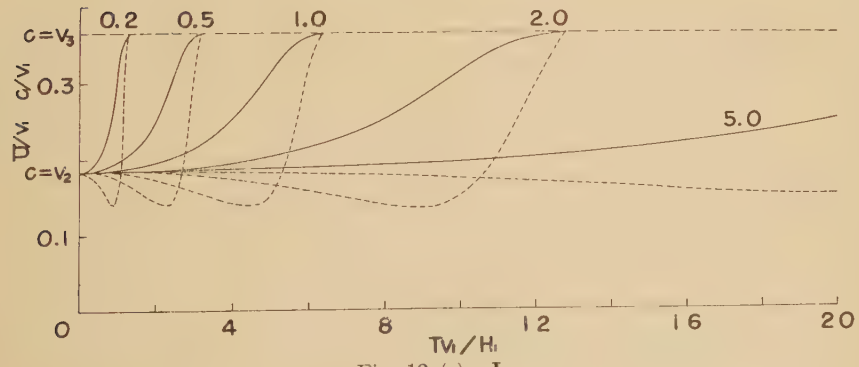

Fig. 12 (a). L_1

Fig. 12 illustrates the first two modes, $\mathbf{L}_0$ and $\mathbf{L}_1$, in the two cases (a) $\mu_2/\mu_1=1/30$, $\mu_3/\mu_2=4$ and (b) $\mu_2/\mu_1=1/30$, $\mu_3/\mu_2=10$, the parameter being H_2/H_1.

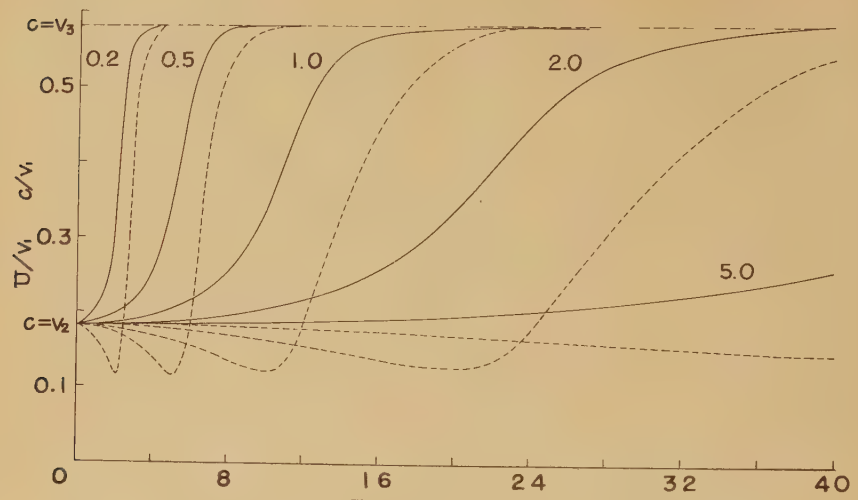

Fig. 12 (b). $\mathbf{L}_0$

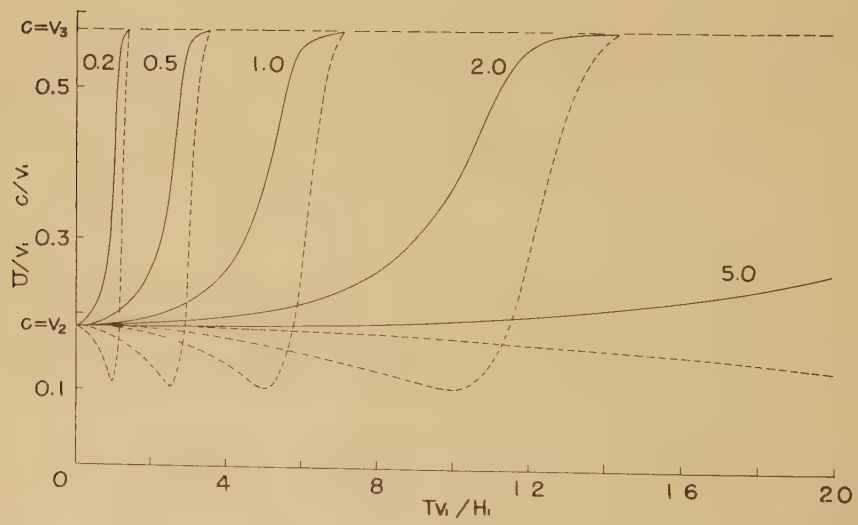

Fig. 12 (b). $\mathbf{L}_1$

Fig. 12. Dispersion curves for $\mathbf{L}_0$ and $\mathbf{L}_1$ in cases (C).
(a) $\mu_2/\mu_1=1/30$ aud $\mu_3/\mu_2=4$, (b) $\mu_2/_1=1/30$ and $\mu_3/\mu_2=10$.

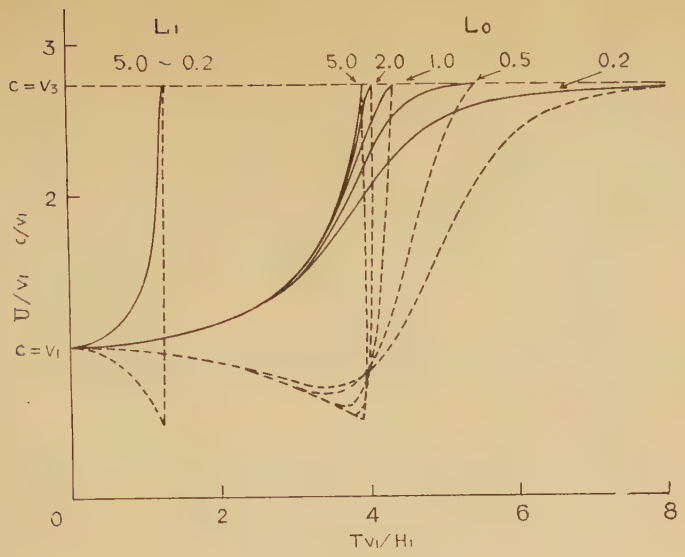

Fig. 13 (a). $\mathbf{L}_0$, $\mathbf{L}_1$

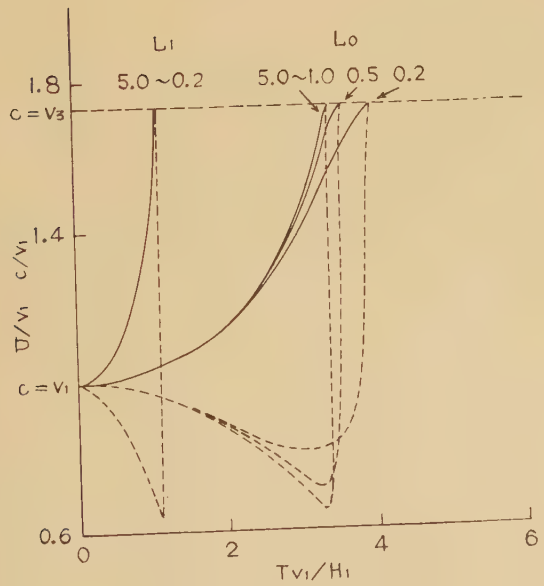

Fig. 13 (b). $\mathbf{L}_0$, $\mathbf{L}_1$

Fig. 13. Dispersion curves for $\mathbf{L}_0$ and $\mathbf{L}_1$ in case (D).
(a) $\mu_2/\mu_1 = 30$ and $\mu_3/\mu_2 = 1/4$, (b) $\mu_2/\mu_1 = 30$ and $\mu_3/\mu_2 = 1/10$.

Case (D) from (57) may take the type (i) in (26). The dispersion curve has been calculated by the characteristic equation (i) in (27). Fig. 13 illustrates the first two modes in the two cases (a) $\mu_2/\mu_1=30$, $\mu_3/\mu_2=1/4$ and (b) $\mu_2/\mu_1=30$, $\mu_3/\mu_2=1/10$, the parameter being H_2/H_1.

In cases (A) and (B), $\mathbf{L}_0$ has no cutoff period. On the other hand in cases (C) and (D), $\mathbf{L}_0$ as well as $\mathbf{L}_1$ has the cutoff period at which phase- and group-velocities coincide respectively with the velocity of S-wave in the lowest layer. The cutoff period must be decreased by increasing the value of H_2/H_1.

In cases (C) and (D) the dispersion curve has only one group velocity minimum, whereas in cases (A) and (B) the curve has two group velocities minimum.

17. Numerical calculations of the amplitude function for $\mathbf{L}_0$ and $\mathbf{L}_1$ in cases (C) and (D)

The results are illustrated in Figs. 14 and 15. The maximum value of

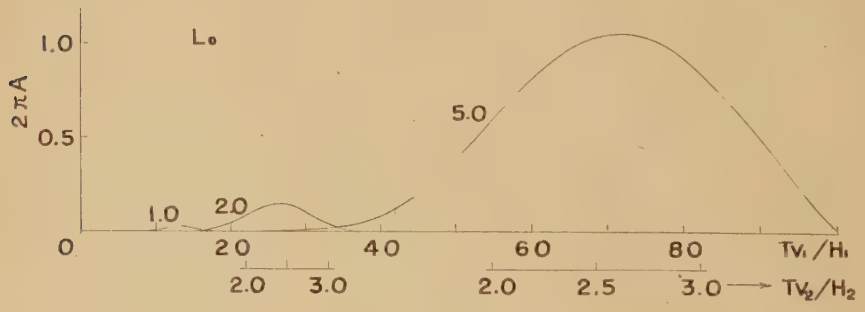

Fig. 14 (a). $\mathbf{L}_0$

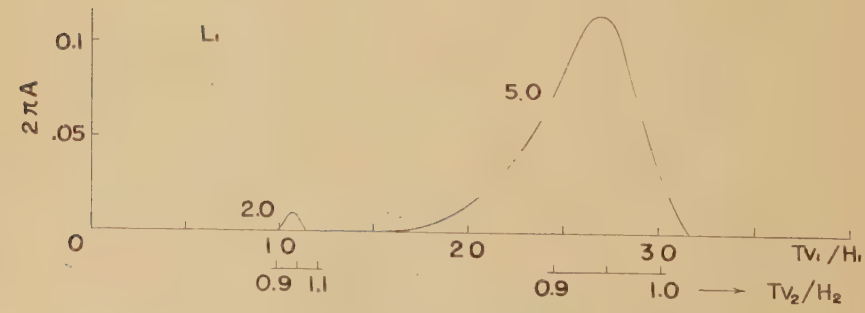

Fig. 14 (a). $\mathbf{L}_1$

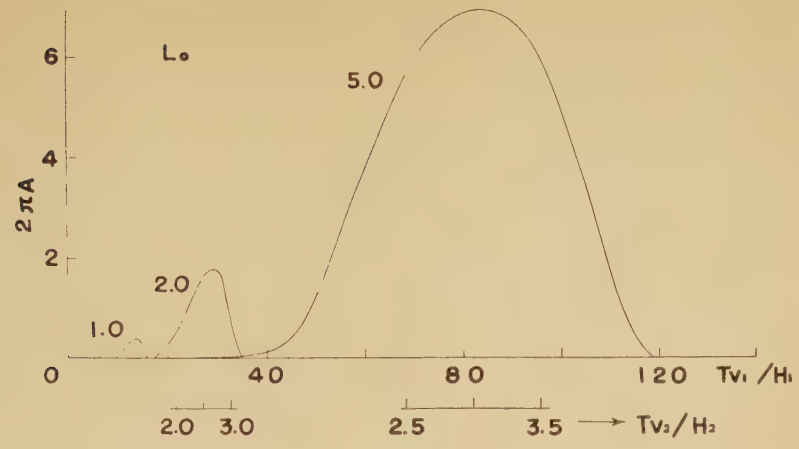

Fig 14 (b). $\mathbf{L}_0$

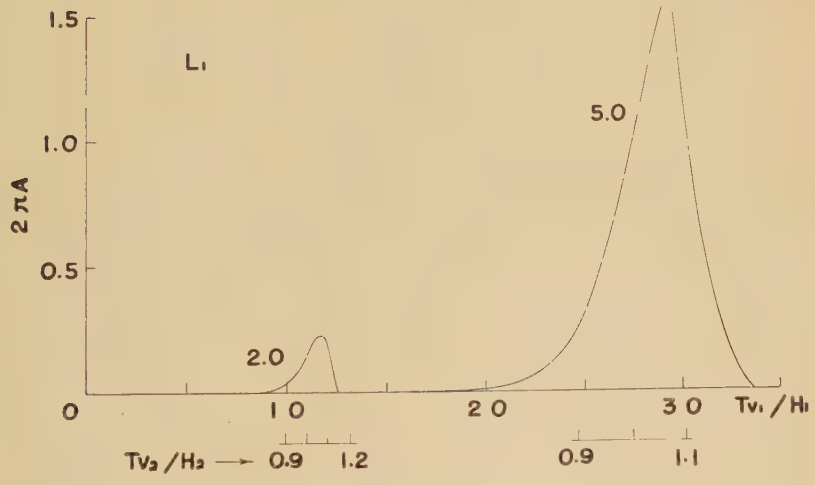

Fig. 14 (b). $\mathbf{L}_1$

Fig. 14. Amplitude functions for $\mathbf{L}_0$ and $\mathbf{L}_1$ in case (C).

the amplitude function is slight when H_2/H_1 is small. However the maximum value increases suddenly with increase of H_2/H_1.

In case (D) the amplitude function for $\mathbf{L}_0$, as shown in Fig. 15, has the maximum near $Tv_1/H_1=4$ and that for $\mathbf{L}_1$ near $Tv_1/H_1=4/3$.

It may be curious that the amplitude function for $\mathbf{L}_1$ in case (D) is not influenced by the ratio H_2/H_1.

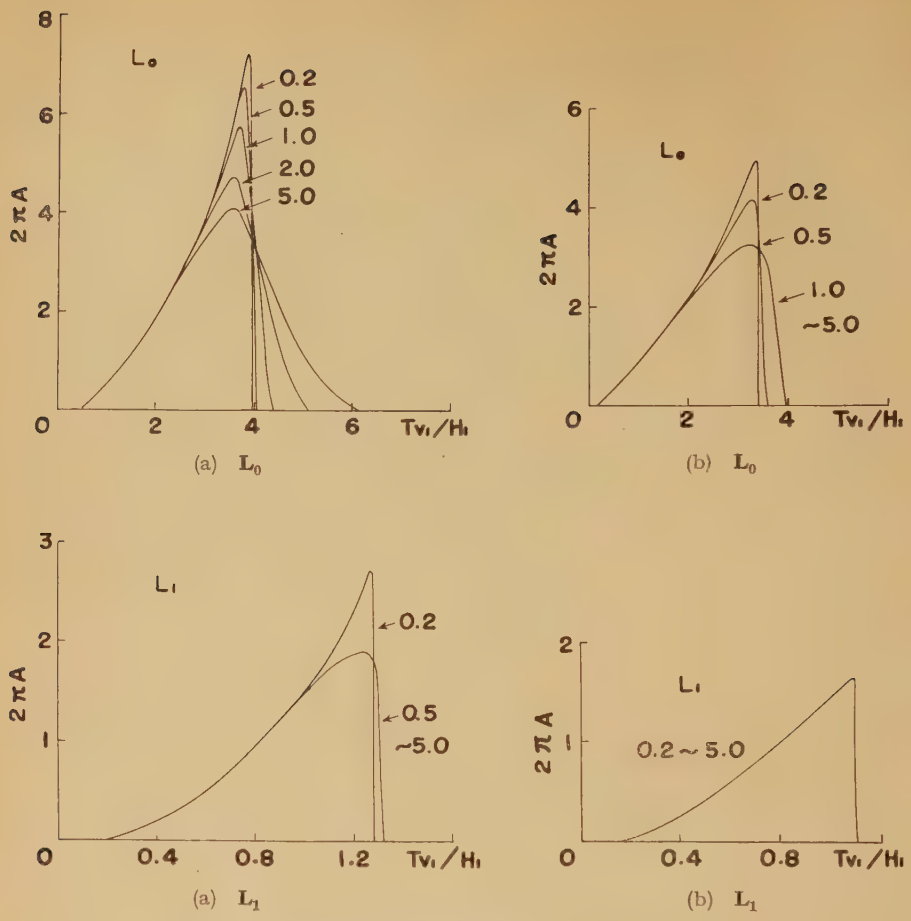

Fig. 15. Amplitude functions for $\mathbf{L}_0$ and $\mathbf{L}_1$ in case (D).

18. Numerical calculations of the amplitude distribution for L_0 and L_1 in cases (C) and (D)

The results are exhibited in Figs. 16 and 17 for several periods indicated by $T/(H_2/v_2)$ or $T/(H_1/v_1)$ respectively.

The amplitude distribution in case (C) may form a type of half wave-length within the second layer, whereas that in case (D) may form a type of quarter wave-length in the first layer.

It must be noted in case (D) that the amplitude in the lowest layer becomes remarkably small, if μ_3/μ_2 decreases or if H_2/H_1 increases.

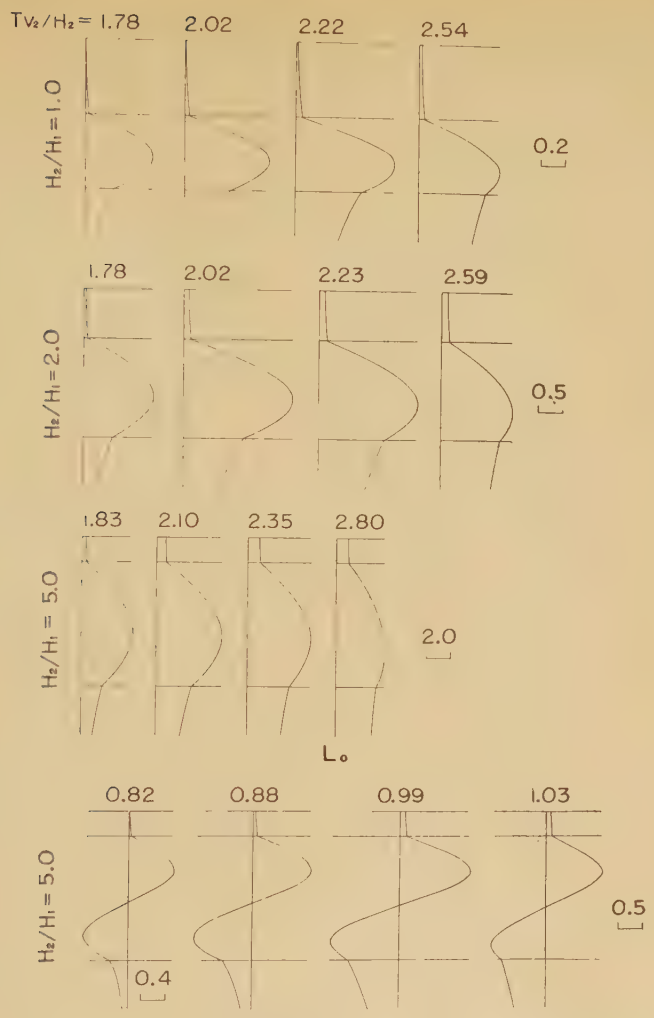

Fig. 16 (a) $\mathbf{L}_0$, $\mathbf{L}_1$

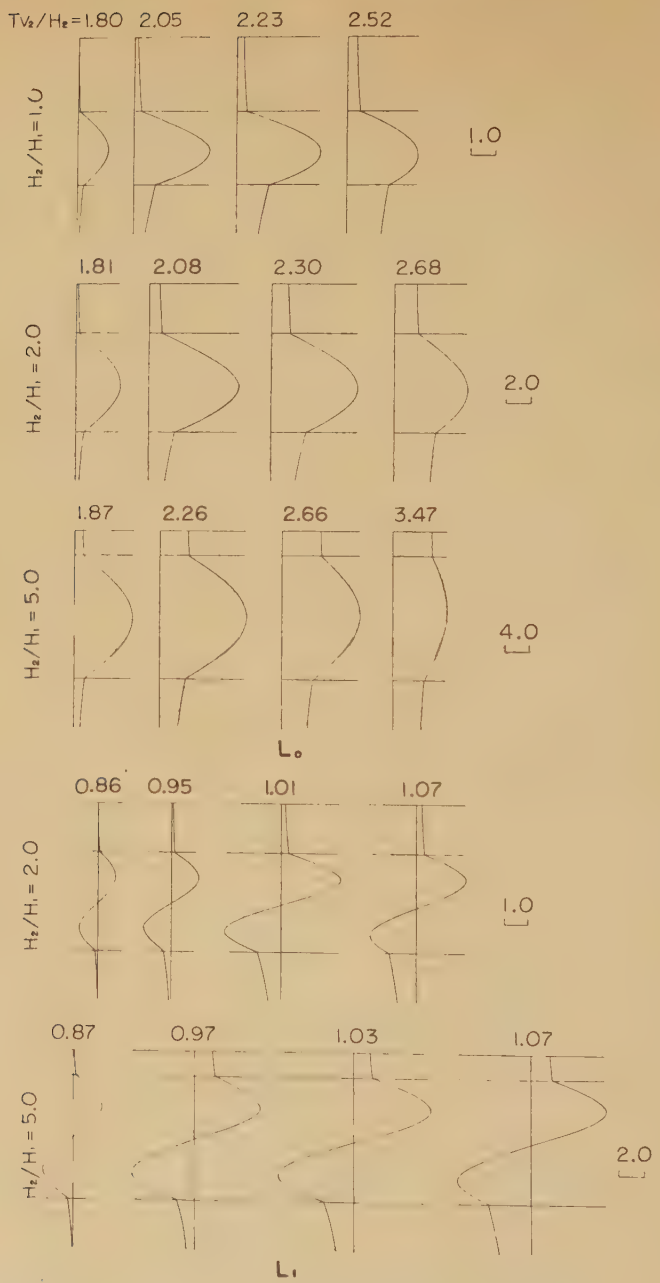

Fig. 16 (b). $\mathbf{L}_0$, $\mathbf{L}_1$

Fig. 16. Amplitude distributions for $\mathbf{L}_0$ and $\mathbf{L}_1$ in case (C).

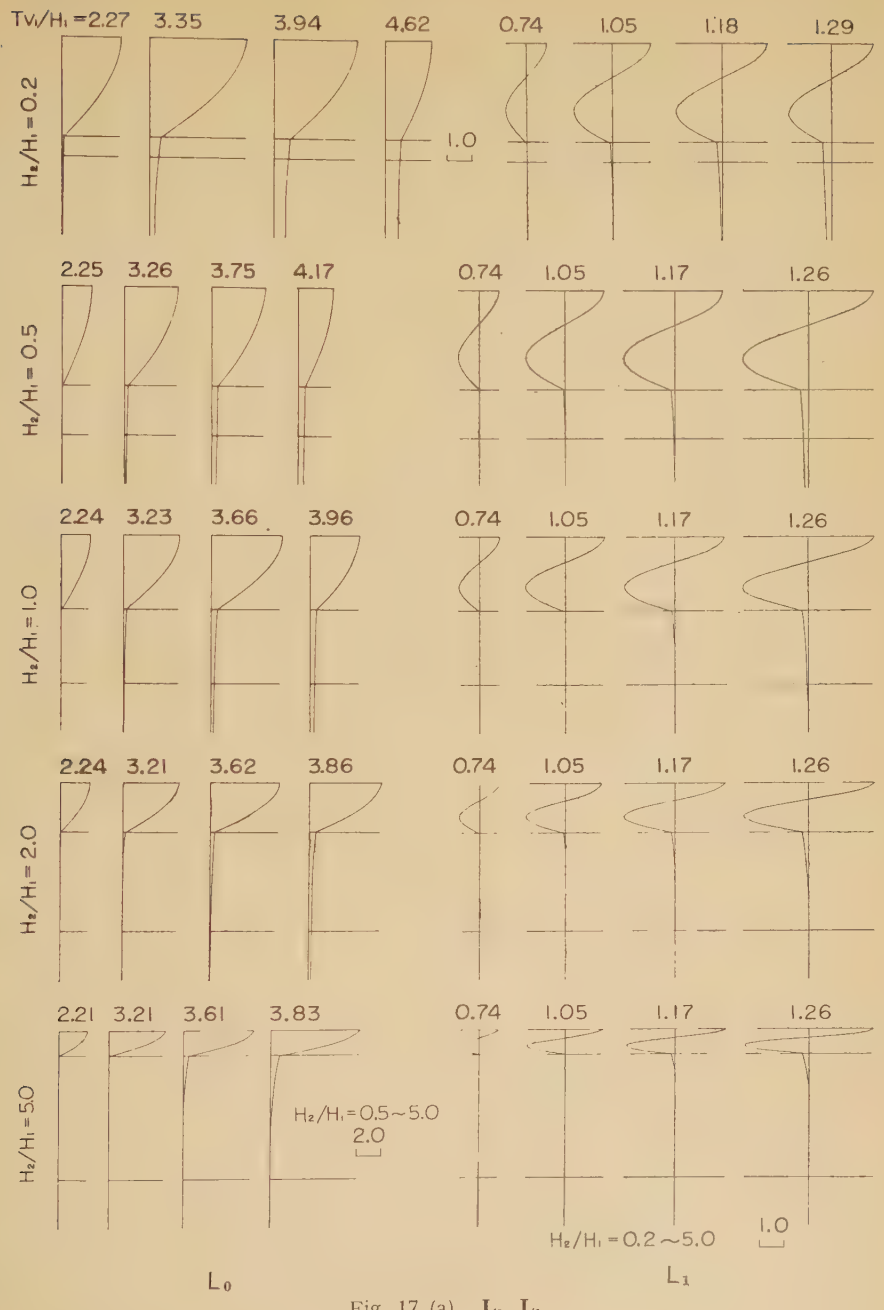

Fig. 17 (a). $\mathbf{L}_0$, $\mathbf{L}_1$

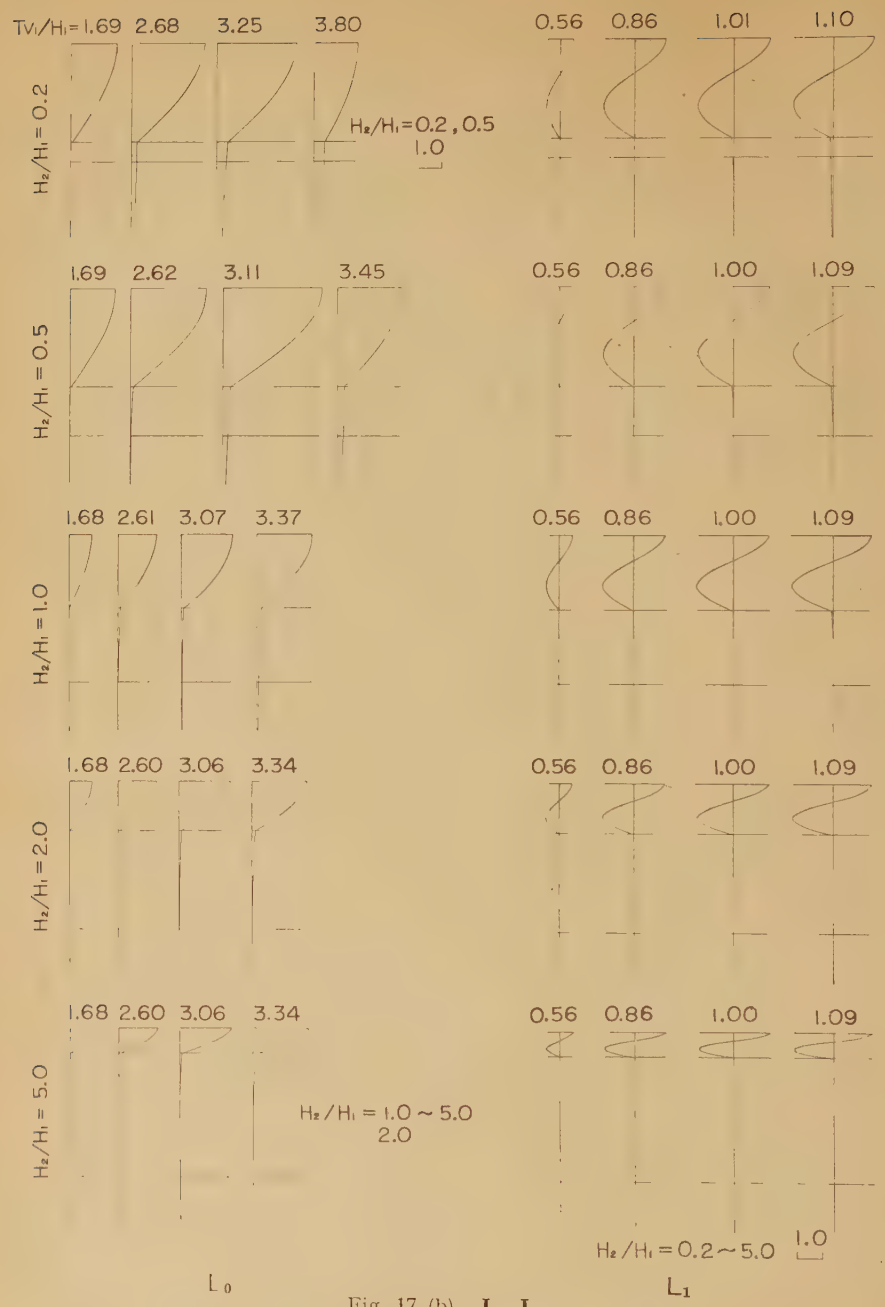

Fig. 17 (b). $\mathbf{L}_0$, $\mathbf{L}_1$

Fig. 17. Amplitude distributions for $\mathbf{L}_0$ and $\mathbf{L}_1$ in case (D).

19. Conclusions

It is the principal aim of this paper to investigate the basic property of LOVE-waves. In order to make the idea concrete, rather large rigidity ratios are assumed in the numerical calculation, regardless of actual conditions of the earth. These large rigidity ratios will be found only near the surface of the earth in seismic prospecting.

"Quarter wave-length law" has been often experienced in actual observations[7)8)]. It has been expected physically that the amplitude of displacement would be large at the phase corresponding to the minimum group velocity. However this expection was too abstract to be connected with that law actually experienced.

If a pulse is generated from a source, the observed displacement must have the factor $\{|dU/d\omega|\}^{-1/2}$, as is well known theoretically[9)10)]. Indeed the displacement of the stationary phase of group velocity will be large, owing to this factor. But the contribution of this facter is not so effective in making the amplitude of the stationary phase larger than that of the other phase.

The present authors have noticed the amplitude function $2\pi A(\xi)$ itself at periodic motion. They have found that the law of (64) was satisfied by the phase corresponding to the maximum of the amplitude function. Due to the factor $(v_1/U-v_1/c)$ contained in $2\pi A(\xi)$, it will be recognized moreover that the minimum group velocity may give the maximum amplitude.

(64) recalls to our minds the vibration of sound in a tube, one end closed. But it was obscure, with this analogy alone, why the period corresponding to the minimum group velocity would satisfy (64). To tell the truth, a quarter wave-length in z-direction is shown by the amplitude distribution more completely at $Tv_1/H_1 \fallingdotseq 0$ than at $Tv_1/H_1 \fallingdotseq 4$. It must be remarked here that the true wave-length in z-direction is $2\pi/\bar{\eta}_1$ and Tv_1 means nothing but an apparent wave-length.

In spite of this physical uncertainty, the acuthors think, the calculated result (64) must be interesting. The observed experience and the abstract consideration, mentioned at the beginning of this section, have been connected well by (64) to each other at least numerically.

In some cases the maximum of the amplitude function is got also near the phase corresponding to the maximum group velocity. This phenomenon is physically less clear than that described already. The low velocity layer must play a grand role in it.

Shielding effect "Quarter wave-length law" is apt to be satisfied by the large

velocity contrast between layers. The nearer the surface of the earth the boundary exists, the larger becomes its effect. If $\mu_2/\mu_1=\mu_3/\mu_2$, for instance, the third layer cannot play an important role but the second layer plays the greatest part. This phenomenon may be recognized by comparison of Fig. 6 (a) with Fig. 6 (b). In Fig. 6 (b) very small energies penetrate into even the second layer. In this circumstance the boundary between the first and the second layers acts as if it were a shielding screen for the lower layers.

In Fig. 6 (a) the subsurface has two screens; one is the boundary between the first and the second layers and the other is that between the second and the third layers. The latter screen is more effective than the former in Fig. 6 (a). Of course, the thicker the layer acting as a screen, the stronger the shielding effect.

Owing to the shielding effect, it will be easy to deduce, by the observation of surface waves, the geological construction near the surface of the earth. On the other hand, deep constructions cannot be deduced from the observation of surface waves, because deep layers must be masked by shallow layers.

Surface waves generated near the surface must be mainly affected by very small constructions near the surface and they will take nearly whole parts of "noise" on the ground.

If the source of the wave lies deep from the surface, only the waves having large wave-length must be taken into account, because the waves having short wave-length have slight amplitude on the ground in this case. This may be understood by Fig. 6, recalling "reciprocal theorem"[1]. Love-waves having as large wave-length as the thickness of the earth's crust have been observed in natural earthquakes[8]. Natural earthquakes have so deep sources that the surface waves having short wave-length which might be affected by small construction near the surface cannot be observed on the ground, no matter how large a velocity contrast exists near the surface of the earth.

Now we will conclude that the first boundary which has a large velocity contrast under the source plays the most important role in growth of Love -waves. To say it in other words, that first boundary alone will be found by the observation of Love-waves.

Acknowledgment The present authors express their thanks to Miss Miyako Murota for her help in numerical calculations. The authors wish again to express their thanks to the Ministry of Education for a grant from the Science Research Fund 1958 by the aid of which the present paper has been published.

References

6) Tazime, K. and Okada, H.: Love-waves in Stratified Three Layers. Journ. Fac. Sci. Hokkaido Univ., Ser. VII, **1** (1958), 115–138.

7) Tazime, K. and Okada, H.: Observation of the Velocity of S-waves near the Surface of the Earth. (In Japanese). Butsuri-tanko, **11** (1958), 65–70.

8) Stoneley, R.: Surface Waves Associated with 20° Discontinuity. M. N. R. A. S. Geophys. Suppl., **4** (1937), 39–43.
Sezawa, K. and Kanai, K.: Relation between the Thickness of a Surface Layer and the Amplitudes of Love-waves. Bull. Earthq. Res. Inst., **15** (1937), 577–581.

9) Jeffreys, H.: Operational Method in Mathematical Physics. C.U.P. (1931), 92–94.

10) Pekeris, C.L.: Theory of Propagation of Explosive Sound in Shallow Water. Geol. Soc. Am., Mem. **27** (1948).

Errata to the previous paper[6)]

Page	Line or expression			
121	(27) (iii)	$\tanh \hat{\eta}_1 H_1 = \tan \hat{\delta}_{12}$	read	$\tanh \hat{\eta}_1 H_1 = -\tan \hat{\delta}_{12}$....
121	last	$\ldots.\coth\left\{\bar{\eta}_1 H_1\left(\frac{\hat{\eta}_2 H_2}{\bar{\eta}_1 H_1}\right)+\hat{\delta}_{22}'\right\}$	〃	$\ldots.\coth\left\{\bar{\eta}_1 H_1\left(\frac{\hat{\eta}_2 H_2}{\bar{\eta}_1 H_1}\right)+\hat{\delta}_{23}'\right\}$
122	(31)	$K_{12} K_{23} \cdot 2i\eta_2 H_2$	〃	$K_{12} K_{23} e^{-2i\eta_2 H_2}$
125	16	$\cosh(\hat{\eta}_2 H_2 + \hat{\delta}_{23})$	〃	$\cosh 2(\hat{\eta}_2 H_2 + \hat{\delta}_{23})$
126	(48)	$\cot \eta_1 H_1 = \frac{\mu_1 \eta_1}{\mu_3 \eta_3} + \ldots.$	〃	$\cot \eta_1 H_1 = \frac{\mu_1 \eta_1}{i \mu_3 \eta_3} + \ldots.$
127	5∼8	It is very easy to .... of Love-waves.		transfer to below line 5 of page 128
127	15	$2\pi A(\xi) = \omega\left(\frac{1}{U}-\frac{1}{c}\right)\cdot\beta'$	read	$2\pi A(\xi) = 2\pi\omega\left(\frac{1}{U}-\frac{1}{c}\right)\cdot\beta'$
127	(52)	$2\pi A(\xi) = \left(\frac{1}{U}-\frac{1}{c}\right)\ldots.$	〃	$2\pi A(\xi) = 2\pi\left(\frac{1}{U}-\frac{1}{c}\right)\ldots.$
127	23∼25	It is very easy to .... for $c=v_3$.		transfer to below line 9 of page 128
129	Fig. 2.(C)	Ordinate 2.0	read	1.5
129	6	$T(v_1/H_1 + v_2/H_2) = 4$	〃	$T/(H_1/v_1 + H_2/v_2) = 4$
138	5	$R_{1,2}$	〃	$\mathcal{R}_{1,2}^{(1)}$

[Journal of the Faculty of Science, Hokkaidô University, Japan, Ser. VII, Vol. I, No. 3, 1959]

Transition from Dispersive RAYLEIGH Waves to Sound Waves in a Layer over a Half Space Absolutely Rigid

Kyozi TAZIME

(Received Sept. 25, 1959)

Abstract

Dispersive RAYLEIGH waves in a layer over a half space absolutely rigid were investigated pretty thoroughly by GIESE[1].

He ignored $\mathbf{M}^{(2)}$-type of the waves, assuming that this type had much smaller amplitude than that of $\mathbf{M}^{(1)}$-type. However the present paper suggests that his assumption had no theoretical foundation.

Moreover he did not refer to any higher order of **M**-waves. Indeed he treated media having POISSON's ratios larger than 0.25, but the character of **M**-waves was obscure at the limit when POISSON's ratio arrived at 0.50.

It is the main purpose of the present paper to clear up the last defect just mentioned.

It must be noted that notations and expressions in this paper will follow those employed and obtained in the previous paper by the present author[2].

1. Superficial waves in a liquid layer

Taking space-coordinates as shown in Fig. 1 and assuming a line source at $z=E$, displacement-potential of superficial waves can be written as

$$[\phi]^{(l)}_{=\mathbf{M}_0} = -\frac{2\pi\omega}{\bar{\alpha}^2 H}\left(\frac{1}{U}-\frac{1}{c}\right)\sin\bar{\alpha}E\,\sin\bar{\alpha}z\,, \tag{1.1}$$

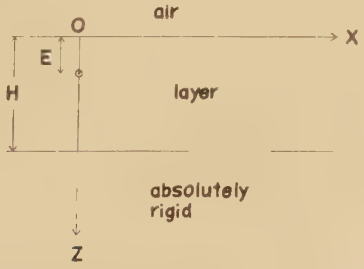

Fig. 1. Space-coordinates under consideration.

being the same expression as that obtained in the case of a plate[3].

In (1.1) the characteristic equation is given by

$$\mathbf{M}^{(l)} = 0 \quad \text{that is} \quad \cos \bar{\alpha} H = 0 \tag{1.2}$$

or

$$\bar{\alpha} H = (2l+1)\pi/2, \ (l = 0, 1, 2, \ \ldots .) . \tag{1.3}$$

2. Dispersive RAYLEIGH waves in a solid layer

In a solid layer, as well known, $\mathbf{M}^{(1)}$ and $\mathbf{M}^{(2)}$-waves must exist. The displacement-potential of them can be expressed, by means of a method similar to that used in a solid plate, as follows.

(i) $c \geqq v_p > v_s$; $\alpha = \bar{\alpha}$, $\beta = \bar{\beta}$.

$$\left.\begin{aligned}
[\phi]_{M=0} = &-\frac{\pi\omega}{\bar{\alpha}^2 H}\left(\frac{1}{U}-\frac{1}{c}\right)\big[\cos\bar{\alpha}(z-E)\{(1-AA')\sin\bar{\alpha}H\cos\bar{\beta}H \\
&+(1+AA')\cos\bar{\alpha}H\sin\bar{\beta}H\}+\sin\bar{\alpha}(z+E)\{-(A-A')\cos\bar{\alpha}H\cos\bar{\beta}H \\
&+(A+A')\sin\bar{\alpha}H\sin\bar{\beta}H\}+\cos\bar{\alpha}(z+E)\{(A-A')\sin\bar{\alpha}H\cos\bar{\beta}H \\
&+(A+A')\cos\bar{\alpha}H\sin\bar{\beta}H\}\big]/N, \\
[\psi]_{M=0} = &\, i\frac{\pi\omega}{\bar{\alpha}^2 H}\left(\frac{1}{U}-\frac{1}{c}\right)\big[B\{(1+A')\cos\bar{\alpha}(E-H)\cos\bar{\beta}(z-H) \\
&-(1-A')\sin\bar{\alpha}(E-H)\sin\bar{\beta}(z-H)\}+B'\{(1+A)\cos\bar{\alpha}E\cos\bar{\beta}z \\
&-(1-A)\sin\bar{\alpha}E\sin\bar{\beta}z\}\big]/N, \\
N = &\{(1-AA')+(\bar{\beta}/\bar{\alpha})(1+AA')\}\sin\bar{\alpha}H\cos\bar{\beta}H+\{(1+AA') \\
&+(\bar{\beta}/\bar{\alpha})(1-AA')\}\cos\bar{\alpha}H\sin\bar{\beta}H,
\end{aligned}\right\} \tag{2.1}$$

in which the characteristic equation is given by

$$\mathbf{M} = 0 \ \text{that is} \quad \sin^2\tfrac{1}{2}(\bar{\alpha}+\bar{\beta})H - AA'\sin^2\tfrac{1}{2}(\bar{\alpha}-\bar{\beta})H = \tfrac{1}{2}(1-AA'-BC') . \tag{2.2}$$

A' in (2.1) and (2.2) means PP-reflecting coefficient as to displacement-potential on the lower boundary in a superficial layer.

Letting rigidity of the layer tend to zero, A must approach to -1 and B to zero, as already mentioned in the case of a plate. On the other hand, A' will approach to 1 at the same time, whichever value phase-velocity may have, as illustrated in Fig. 2. B' as well as C' will approach to zero again, being $B'^2 = (\bar{\alpha}/\bar{\beta})(1-A'^2)$. In this case, $[\psi]_{M=0}$ in (2.1) must be zero and (2.2) will be reduced to

$$\{(\tan\bar{\alpha}H/2-1)(\tan\bar{\beta}H/2+1)\}\{(\tan\bar{\alpha}H/2+1)(\tan\bar{\beta}H/2-1)\} = 0 , \tag{2.3}$$

that is

$$\bar{\alpha}H = (2l+1)\pi/2 \quad \text{or} \quad \bar{\beta}H = (2m+1)\pi/2 , \tag{2.4}$$

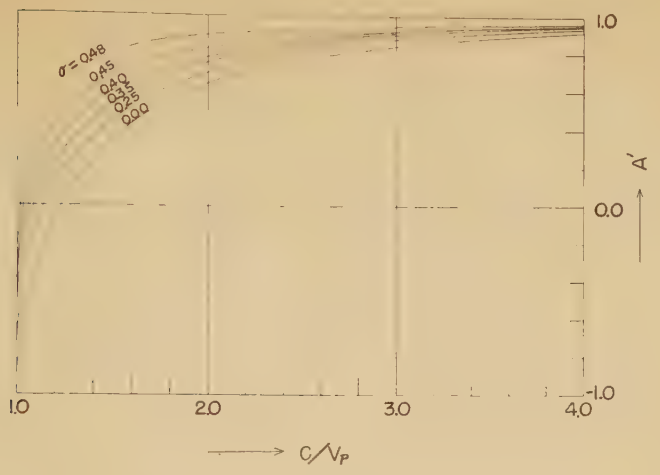

Fig. 2. PP-reflecting coefficient on the lower boundary in a layer.

where l and m represent positive integers, indicating orders of these curves. The former of (2.4) coincide with (1.3) and one sees that $[\phi]_{M=0}$ in (2.1) will coincide with that in (1.1).

On the other hand, when the latter of (2.4) is satisfied, $[\psi]_{M=0}$ in (2.1) must be zero.

Thus letting rigidity of the layer tend to zero, branches corresponding to $(\tan \bar{\alpha}H/2-1)(\tan \bar{\alpha}H/2+1)=0$ alone can survive, otherwise amplitudes of displacement-potentials become zero. The surviving two branches coincide respectively with the branches of the even and odd orders of superficial waves in a liquid layer.

(ii) $v_p \geqq c \geqq v_s$; $\alpha = -i\hat{\alpha}$, $\beta = \hat{\beta}$.

$$
\left.
\begin{aligned}
[\phi]_{M=0} &= \frac{\pi\omega}{\hat{\alpha}^2 H}\left(\frac{1}{U}-\frac{1}{c}\right)\left[\cosh \hat{\alpha}(z-E)\left\{e^{\hat{\alpha}H}\sin(\bar{\beta}H-\delta-\delta)\right.\right.\\
&\quad \left.+e^{-\hat{\alpha}H}\sin(\bar{\beta}H+\delta+\delta)\right\}-\left\{e^{\hat{\alpha}(z+E-H)}\sin(\bar{\beta}H-\delta-\delta)\right.\\
&\quad \left.\left.+e^{-\hat{\alpha}(z+E-H)}\sin(\bar{\beta}H+\delta-\delta)\right\}\right]/N,\\
[\psi]_{M=0} &= i\frac{\pi\omega}{\hat{\alpha}^2 H}\left(\frac{1}{U}-\frac{1}{c}\right)\left(\frac{2\hat{\alpha}}{\bar{\beta}}\right)\left[(\sin 2\delta)^{1/2}\left\{e^{\hat{\alpha}(E-H)}\sin(\beta(z-H)-\delta)\right.\right.\\
&\quad \left.-e^{-\hat{\alpha}(E-H)}\sin(\bar{\beta}(z-H)+\delta')\right\}+(\sin 2\delta')^{1/2}\left\{e^{\hat{\alpha}E}\sin(\bar{\beta}z-\delta)\right.\\
&\quad \left.\left.-e^{-\hat{\alpha}E}\sin(\bar{\beta}z+\delta)\right\}\right]/N,\\
N &= e^{\hat{\alpha}H}\sin(\bar{\beta}H-\delta-\delta')+e^{-\hat{\alpha}H}\sin(\bar{\beta}H+\delta+\delta')\\
&\quad +(\bar{\beta}/\hat{\alpha})\left\{e^{\hat{\alpha}H}\cos(\bar{\beta}H-\delta-\delta')-e^{-\hat{\alpha}H}\cos(\bar{\beta}H+\delta+\delta')\right\},
\end{aligned}
\right\} \quad (2.5)
$$

in which the characteristic equation is given by

$$\mathbf{M} = 0 \text{ that is}$$

$$\left\{e^{\hat{\alpha}H/2}\cos\tfrac{1}{2}(\bar{\beta}H-\delta-\delta')-e^{-\hat{\alpha}H/2}\cos\tfrac{1}{2}(\bar{\beta}H+\delta+\delta')\right\}$$
$$\cdot\left\{e^{\hat{\alpha}H/2}\sin\tfrac{1}{2}(\bar{\beta}H-\delta-\delta)+e^{-\hat{\alpha}H/2}\sin\tfrac{1}{2}(\bar{\beta}H+\delta+\delta')\right\}$$
$$=\sin(\delta+\delta')\pm\left\{\sin^2(\delta+\delta')-\sin^2(\delta-\delta')\right\}^{1/2}. \qquad (2.6)$$

δ' in (2.5) and (2.6) means phase-lag of displacement-potential at PP -reflection on the lower boundary of the layer. Letting rigidity of the layer tend to zero, δ must approach to zero, as already mentioned in the case of a plate. On the other hand, δ' will approach to $\pi/2$ for all values of phase -velocity between v_p and v_s as illustrated in Fig. 3. In this case, $[\psi]_{M=0}$ in (2.5) must be zero and (2.6) will be reduced to

$$\cosh\hat{\alpha}H\ \cos\bar{\beta}H=0. \qquad (2.7)$$

Because $\cosh\hat{\alpha}H$ cannot be zero, $\cos\bar{\beta}H$ must always be zero. Owing to

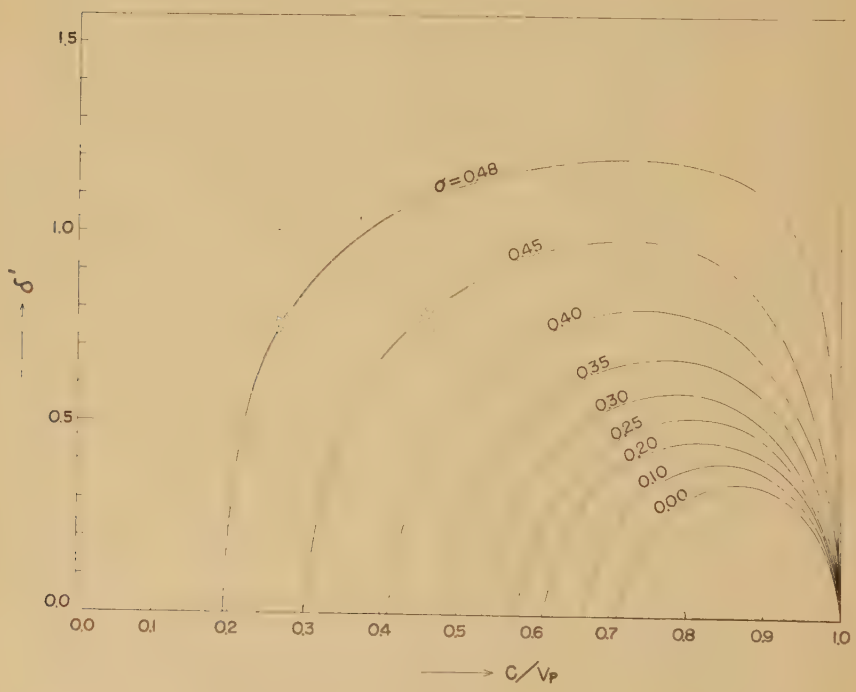

Fig. 3. Phase-lag at PP-reflection on the lower boundary.

this result, one sees that $[\phi]_{M-0}$ in (2.5) also becomes zero. No wave, therefore, can survive in the present case.

(iii) $v_p > v_s \geqq c\,;\ \alpha = -i\,\mathfrak{a}\,,\ \beta = -i\hat{\beta}\,.$

$$
\left.
\begin{aligned}
[\phi]_{M\,0} = {} & -i\,\frac{\pi\omega}{\mathfrak{a}^2 H}\left(\frac{1}{U}-\frac{1}{c}\right)\big[\cosh\mathfrak{a}\,(z-E)\{(1-AA')\sinh\mathfrak{a}H\cosh\hat{\beta}H \\
& +(1+AA')\cosh\mathfrak{a}H\sinh\hat{\beta}H\} - \sinh\mathfrak{a}\,(z+E) \\
& \cdot\{(A-A')\cosh\mathfrak{a}H\cosh\hat{\beta}H+(A+A')\sinh\mathfrak{a}H\sinh\hat{\beta}H\} \\
& +\cosh\mathfrak{a}\,(z+E)\{(A-A')\sinh\mathfrak{a}H\cosh\hat{\beta}H \\
& +(A+A')\cosh\mathfrak{a}H\sinh\hat{\beta}H\}\big]/N, \\
[\psi]_{M=0} = {} & -i\,\frac{\pi\omega}{\mathfrak{a}^2 H}\left(\frac{1}{U}-\frac{1}{c}\right)\big[B\{(1+A')\cosh\mathfrak{a}\,(E-H)\cosh\hat{\beta}\,(z-H) \\
& +(1-A')\sinh\mathfrak{a}\,(E-H)\sinh\hat{\beta}\,(z-H)\}+B'\{(1+A)\cosh\mathfrak{a}E \\
& \cdot\cosh\hat{\beta}z+(1-A)\sinh\mathfrak{a}E\sinh\hat{\beta}z\}\big]/N\,, \\
N = {} & -i\big[\{(1-AA')+(\hat{\beta}/\mathfrak{a})(1+AA')\}\sinh\mathfrak{a}H\cosh\hat{\beta}H \\
& +\{(1+AA')+(\hat{\beta}/\mathfrak{a})(1-AA')\cosh\mathfrak{a}H\sinh\hat{\beta}H\,,
\end{aligned}
\right\} \quad (2.8)
$$

in which the characteristic equation is given by

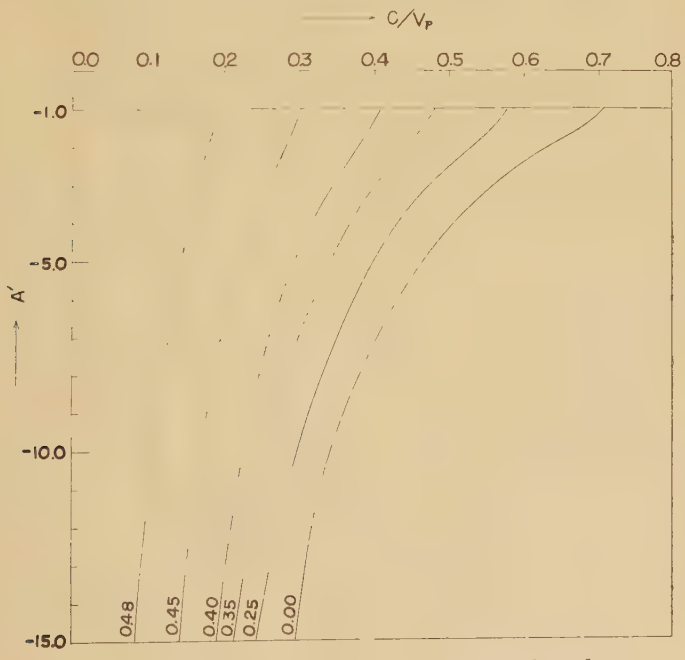

Fig. 4. PP-reflecting coefficient on the lower boundary.

$\mathbf{M}=0$ that is

$$\sinh^2 \tfrac{1}{2}(\mathfrak{a}+\hat{\beta})H - A\dot{A}'\sinh^2 \tfrac{1}{2}(\mathfrak{a}-\hat{\beta})H = \tfrac{1}{2}(BC'+AA'-1) = l^2 . \qquad (2.9)$$

A' in (2.8) and (2.9) means again PP-reflecting coefficient on the lower boundary of the layer.

Letting rigidity of the layer tend to zero, A must be confined to -1, as already mentioned in the case of a plate. On the other hand, A' is to be confined also to -1, as illustrated in Fig. 4. Because B and B' are again zero in this case, $[\psi]_{M=0}$ in (2.8) must be zero and (2.9) will be reduced to

$$\cosh(\mathfrak{a}H/2)\sinh(\hat{\beta}H/2)\sinh(\mathfrak{a}H/2)\cosh(\hat{\beta}H/2) = 0 . \qquad (2.10)$$

As $\cosh(\mathfrak{a}H/2)\sinh(\mathfrak{a}H/2)\cosh(\hat{\beta}H/2)$ cannot be zero, $\sinh(\hat{\beta}H/2)$ must be zero, with the result that $[\phi]_{M=0}$ in (2.8) is also zero.

It has been recognized in this section that dispersive RAYLEIGH waves in a solid layer should be reduced to superficial waves in a liquid layer at the limit when rigidity is taken as zero. In the following section, processes of transition will be investigated.

3. Numerical calculations of the dispersion-curves for various POISSON's ratios

At the limit when POISSON's ratio arrives at 0.50, A' in Fig. 2 must coincide with 1 and A with -1 for any value of c/v_p.

Turning attention to A' and A for general POISSON's ratio, one sees that A' will always approach again to 1 and A to -1 if $c/v_p \gg 1$.

Considering the above two circumstances with Fig. 2, it may be expected that the nearer σ approaches to 0.50, the wider becomes the range satisfying (2.3).

If $c/v_p=1$, one sees $A'=A=-1$ for any value of σ, with the result that the right hand side of (2.2) becomes zero, because $BC'=0$ in this case. Namely one has

$$\sin \mathfrak{a}H \sin \bar{\beta}H = 0 ,$$

being the same as the relation in the case of a plate.

If $c/v_s=1$, one sees again $A'=A=-1$ for any value of σ. Thus one has

$$\sinh \mathfrak{a}H \sin \bar{\beta}H = 0 .$$

Because $\sinh \mathfrak{a}H$ cannot be zero in this case, dispersion-curves must always approach to $\sin \bar{\beta}H=0$ near $c=v_s$.

As one has seen by now, for any value of σ,

$$\cos \bar{\alpha} H = 0 \quad \text{and} \quad \cos \bar{\beta} H = 0 \tag{3.1}$$

might be the bases with respect to dispersion-curves of RAYLEIGH waves in a layer resting on a half space absolutely rigid, if $c/v_p > 1$. On the other hand,

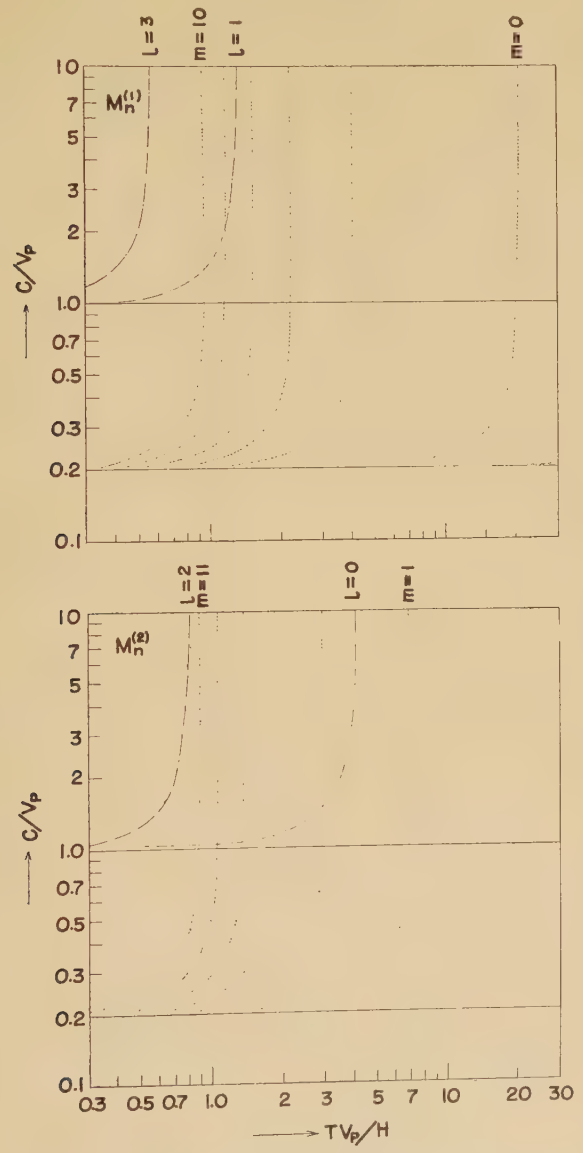

Fig. 5. Chain-lines correspond to $\bar{\alpha}H = (2l+1)\pi/2$, while dotted lines to $\bar{\beta}H = (2m+1)\ \pi/2$. $\sigma = 0.48$.

$$\sin \bar{\beta} H = 0 \tag{3.2}$$

might be the base near $c \doteqdot v_s$.

In Fig. 5 are shown the curves given by (3.1), that is (2.4). Classification of $\mathbf{M}^{(1)}$ and $\mathbf{M}^{(2)}$ in Fig. 5 follows that in the case of a plate. Odd l and even m belong to $\mathbf{M}^{(1)}$, on the contrary even l and odd m to $\mathbf{M}^{(2)}$. The curves given by $\cos \bar{\beta} H = 0$ must be shifted to the rightward with increase in σ, though the curves given by $\cos \bar{\alpha} H = 0$ need not. In Fig. 5, for an example, the curves for $\sigma = 0.48$ are exhibited.

(i) Now $l^2 = \frac{1}{2}(1 - AA' - BC')$ in (2.2) has been calculated at first and is illustrated in Fig. 6. If $c/v_p \gg 1$, one sees that l is equal to unity for any value of σ and (2.2) may be resolved into the next two branches:

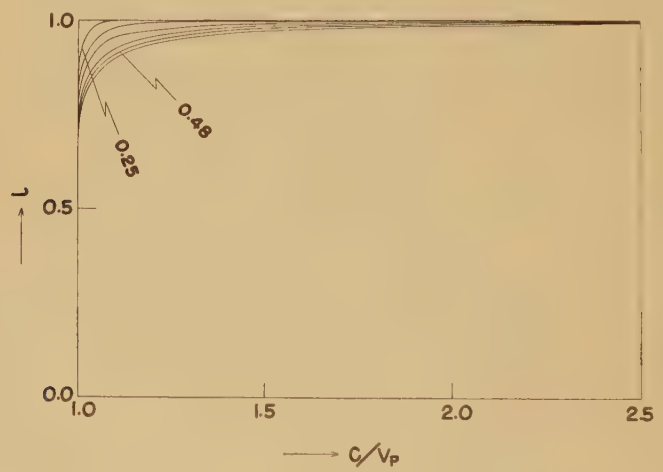

Fig. 6. The relation between l in (2.2) and c/v_p.

$$\left.\begin{aligned} &\cos\left(\frac{\bar{\beta}}{\xi} + \frac{\bar{\alpha}}{\xi}\right)\frac{\xi H}{2} + (-AA')^{1/2} \sin\left(\frac{\bar{\beta}}{\xi} - \frac{\bar{\alpha}}{\xi}\right)\frac{\xi H}{2} = 0 \quad \text{for } \mathbf{M}^{(1)}, \\ &\cos\left(\frac{\bar{\beta}}{\xi} + \frac{\bar{\alpha}}{\xi}\right)\frac{\xi H}{2} - (-AA')^{1/2} \sin\left(\frac{\bar{\beta}}{\xi} - \frac{\bar{\alpha}}{\xi}\right)\frac{\xi H}{2} = 0 \quad \text{for } \mathbf{M}^{(2)}, \end{aligned}\right\} \tag{3.3}$$

where classification of $\mathbf{M}^{(1)}$ and $\mathbf{M}^{(2)}$ depends on the limit when (3.3) will coincide with (2.3) in which $A = -1$ and $A' = 1$. It will be very easy, as in the case of a plate, to obtain dispersion-curves from (3.3).

If c/v_p approaches to 1, l differs from unity and (2.2) cannot be resolved into factors. The process of graphical solution for this case, or

$$\sin\left(\frac{\bar{\beta}}{\xi} + \frac{\bar{\alpha}}{\xi}\right)\frac{\xi H}{2} = \pm\left\{l^2 + AA' \sin^2\left(\frac{\bar{\beta}}{\xi} - \frac{\bar{\alpha}}{\xi}\right)\frac{\xi H}{2}\right\}^{1/2} \tag{3.4}$$

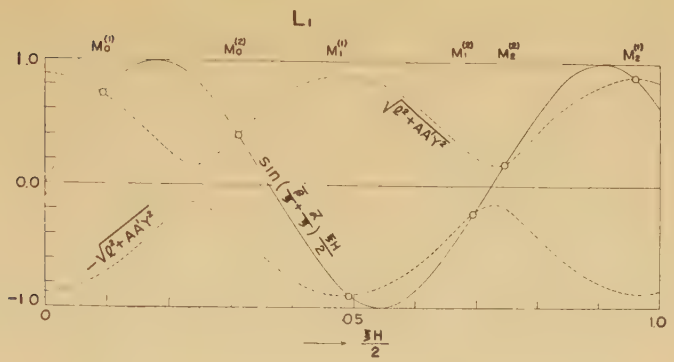

Fig. 7. An example of graphical solutions for (2.2).
$\sigma=0.48$ and $c/v_p=1.5$.

is shown by Fig. 7. Owing to intersection of $\cos\bar{\alpha}H=0$ with $\cos\bar{\beta}H=0$, systematic classification of $\mathbf{M}^{(1)}$ and $\mathbf{M}^{(2)}$ is somewhat disturbed, if c/v_p is not much larger than unity. This disturbance appears in Fig. 7 between $\mathbf{M}_1^{(2)}$ and $\mathbf{M}_2^{(2)}$.

(ii) (2.6) may be rewritten by

$$\sin(\bar{\beta}H-\delta-\delta')=e^{-2\bar{\alpha}H}\sin(\bar{\beta}H+\delta+\delta')\pm 2\,e^{-\bar{\alpha}H}(\sin 2\,\delta\sin 2\,\delta')^{1/2}$$
$$\text{for } c/v_s\gtrless\sqrt{2}\,. \qquad (3.5)$$

An example of graphical solution for (3.5) is exhibited in Fig. 8 where $\mathbf{M}_n^{(1)}$ and $\mathbf{M}_n^{(2)}$ appear in turn regularly, because $\cos\bar{\alpha}H=0$ does not exist in the present region and no disturbance can occur.

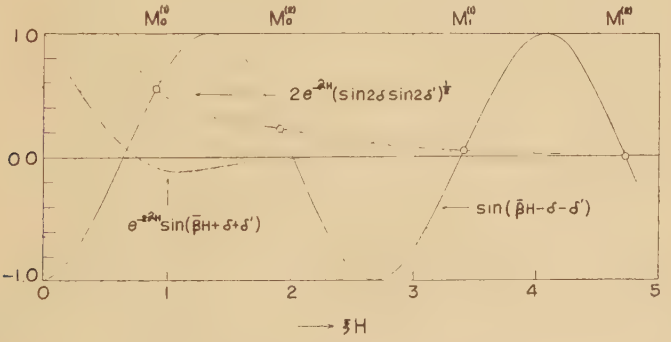

Fig. 8. An example of graphical solution for (3.5).
$\sigma=0.48$ and $c/v_p=0.50$.

If $c/v_p>1$, it cannot be expected to be possible to classify the branch by Fig. 7 alone. In order to avoid this difficulty, Fig. 5 and Fig. 8 must be compared with Fig. 7.

(iii) (2.9) may be rewritten by

$$\sinh\left(\frac{\hat{\alpha}}{\xi}+\frac{\hat{\beta}}{\xi}\right)\frac{\xi H}{2}=\left\{l^2+AA'\sinh^2\left(\frac{\hat{\alpha}}{\xi}-\frac{\hat{\beta}}{\xi}\right)\frac{\xi H}{2}\right\}^{1/2} \tag{3.6}$$

from which $\mathbf{M}_0^{(1)}$ alone will be obtained.

If c becomes smaller than v_s, A and A' will decrease to become remarkably smaller than -1 at once and l^2 in (2.9) will coincide with AA'. In this case (3.6) will be reduced to

$$\sinh\left(\frac{\hat{\alpha}}{\xi}+\frac{\hat{\beta}}{\xi}\right)\frac{\xi H}{2}=l\cosh\left(\frac{\hat{\alpha}}{\xi}-\frac{\hat{\beta}}{\xi}\right)\frac{\xi H}{2}. \tag{3.7}$$

As l in (2.9) is illustrated in Fig. 9, graphical solution of (3.7) is very easy.

Thus the dispersion-curves for $\sigma=0.48$ have been obtained, as shown by full lines in Fig. 10 where the other lines correspond respectively to those in

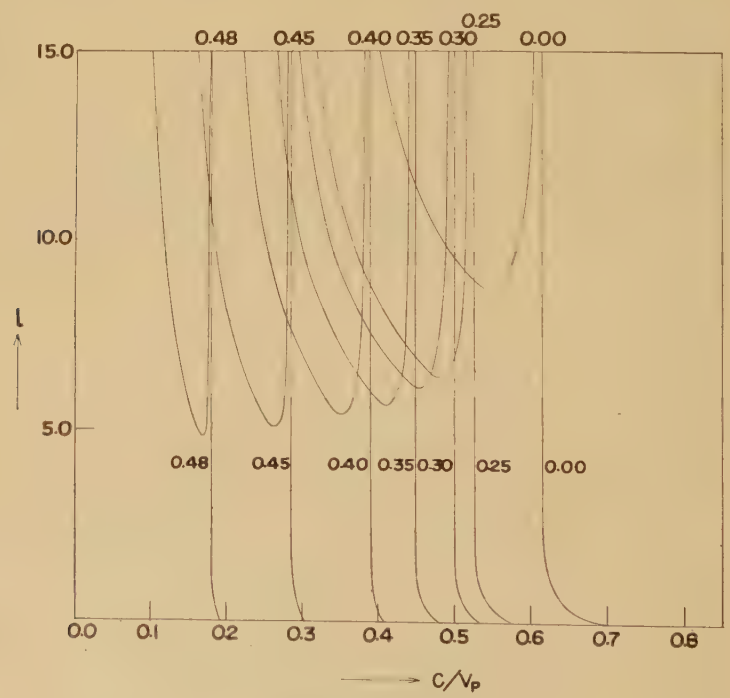

Fig. 9. l in (2.9).

Fig. 5. Dispersion-curves for the other POISSON's ratios are also shown in Figs. 11 to 14 in the same manner as those in Fig. 10.

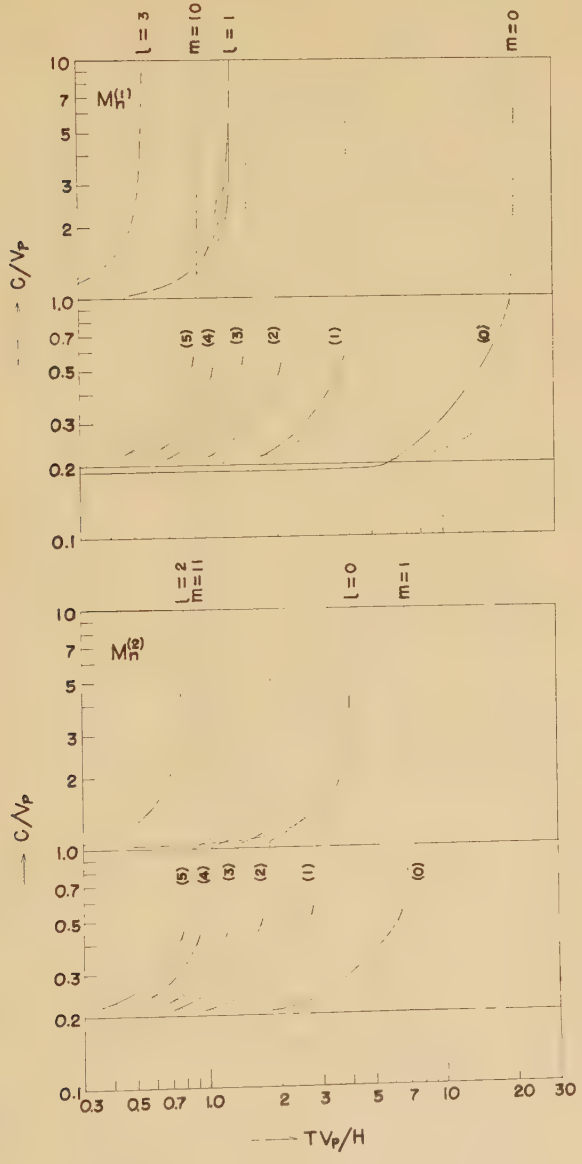

Fig. 10. Dispersion-curves for $\sigma = 0.48$.

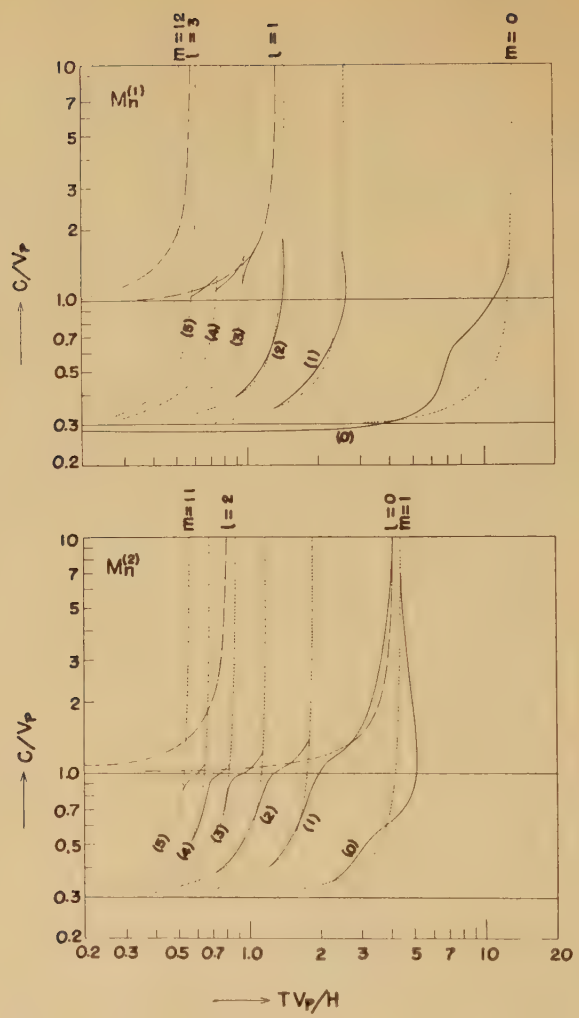

Fig. 11. Dispersion-curves for $\sigma=0.45$.

4. Conclusions

(1) If $c/v_p \gg 1$, the dispersion-curves always coincide with any one of the curves given by (2.4), whatever value σ may have.

(2) If $c/v_p \gg 1$, periods of the former and of the latter equation in (2.4) should coincide with each other under the next condition,

$$2m+1=(2l+1)(v_p/v_s)\,. \tag{4.1}$$

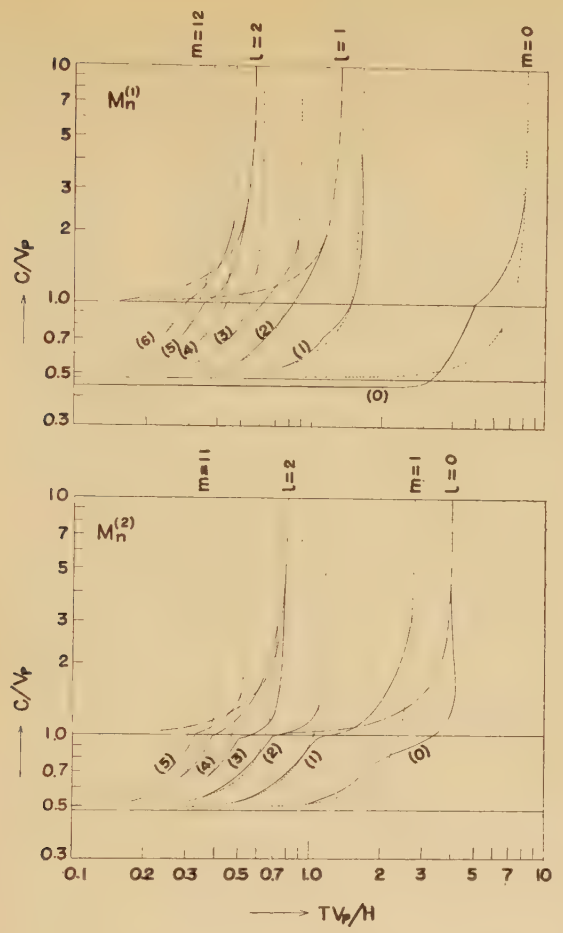

Fig. 12. Dispersion-curves for σ=0.35.

Because odd orders of m must correspond to even orders of l, the lowest order of m satisfying (4.1) is 1 for l=0, resulting in v_p/v_s=3.0 or σ=0.44.

If σ<0.44, no curve indicated by m exists to the right of the curve indicated by l=0 with which $\mathbf{M}_0^{(2)}$ always coincides in this case.

If σ>0.44, on the other hand, some curves indicated by m appear to the right of l=0. The nearer σ approaches to 0.50, the larger becomes the number of m-curves to the right of l=0.

(3) On dotted lines in Fig. 10 to 14 amplitudes of displacement-potentials are zero, though the dispersion-curves may be calculated.

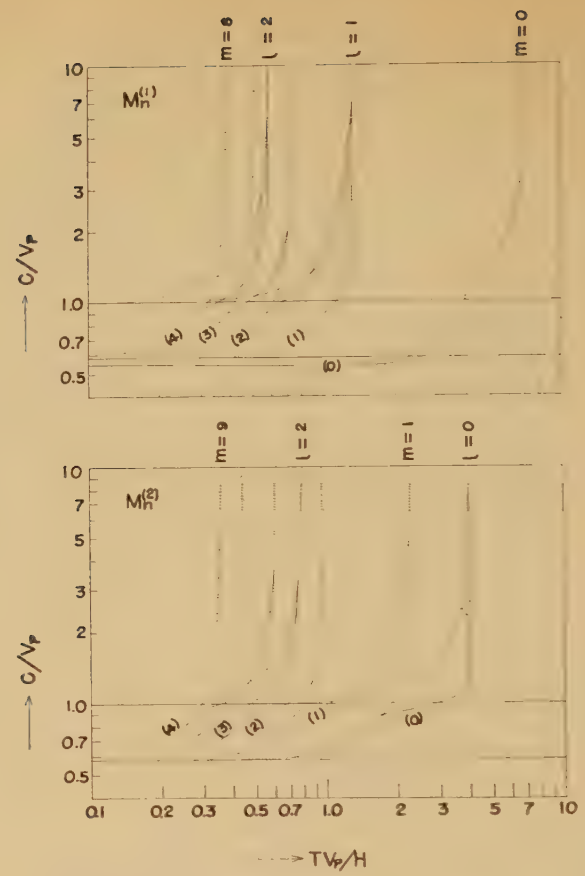

Fig. 13. Dispersion-curves for $\sigma=0.25$.

(4) It may be expected, on the other hand, that on chain-lines amplitudes will be large. Indeed amplitudes on full lines differ from zero, but the maximum amplitude must be attained on chain-lines at

$$Tv_p/H = 4/(2l+1)\,. \tag{4.2}$$

(5) It has been found to be wrong, if $\sigma>0.44$ for $\mathbf{M}_n^{(2)}$ and if $\sigma>0.22$ for $\mathbf{M}_n^{(1)}$, to say that the lower the order of dispersive RAYLEIGH waves is, the larger may become the amplitude of the wave. This situation is completely different from the case of LOVE waves and of sound waves, consisting respectively of either S or P-waves alone.

(6) (4.2) means "quarter wave-length law". It was a wonder that such

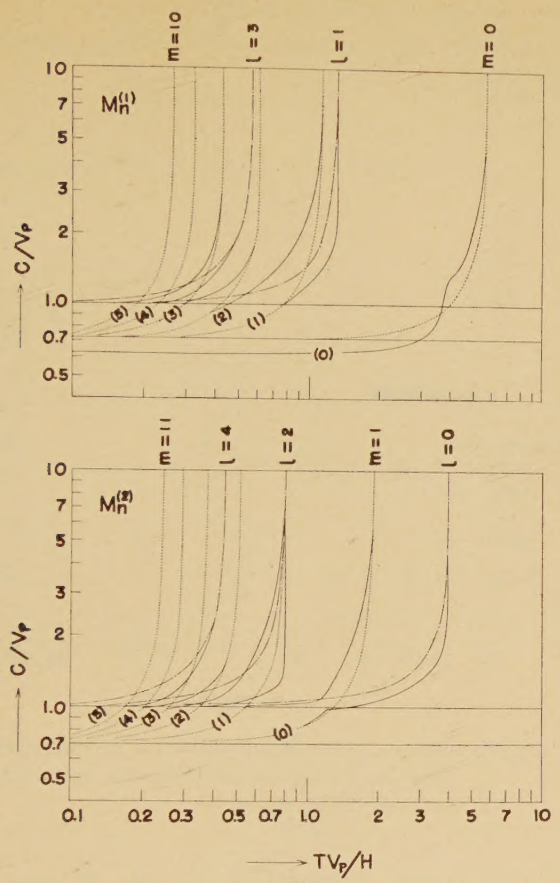

Fig. 14. Dispersion-curves for $\sigma=0.00$.

a law as (4.2) had been often experienced[4] for dispersive RAYLEIGH waves in field-experiments, in spite of the existence of P-wave as well as of S-wave in the layer. But it has been understood in the present paper that among many branches of dispersive RAYLEIGH waves a few of them must correspond to $\cos \bar{\alpha}H=0$ and others to $\cos \bar{\beta}H=0$. Amplitudes of the latter ones cannot be so large that the law containing v_p alone will become important. It must be also noticed that the order of dispersive RAYLEIGH waves cannot be determined from the observed "wave-length law".

(7) Picking out $\mathbf{M}_0^{(1)}$, $\mathbf{M}_0^{(2)}$ and the curve for $l=0$ alone from Figs. 10 to 14, one will obtain Fig. 15. In this figure $\mathbf{M}_0^{(1)}$ and $\mathbf{M}_0^{(2)}$ diverge from the curve for $l=0$ when σ approaches to 0.50. Thus it should not be expected

that two curves, for solid and for liquid waves, will coincide with each other at the limit of $\sigma=0.50$. The process of transition from solid to liquid cannot be understood by Fig. 15.

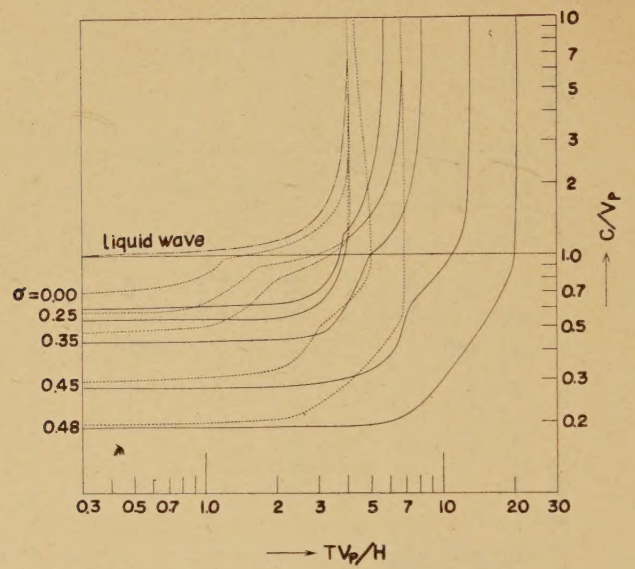

Fig. 15. Comparison of dispersion-curves for the zeroth order of M-waves to the curve for the zeroth order of liquid waves.

According to the present investigation, one sees, the process is very complicated. When σ approaches to 0.50, the zeroth order of liquid waves is constructed approximately of many higher orders $\mathbf{M}_n^{(2)}$-waves and the first order of liquid waves is approximately constructed of many higher orders of $\mathbf{M}_n^{(1)}$-waves and so on.

5. Remarks

If attention is confined in the region of $Tv_p/H \ll 1$ and $c/v_p \approx 1$ in Fig. 5, a similar lattice to MINDLIN's[5] may be formed. The dispersion-curve in this region takes also "terrace-like structure" named by MINDLIN in the case of a plate.

Acknowledgment. The author expresses his thanks to Mr. Toshihiro HIGASHIYAMA, Mr. Makoto KISHI and Miss Miyako MUROTA for their helps in numerical calculations. The author wishes again to express his thanks to Ministry of Education for a grant from the Science Research Fund 1958 by the aid of which the present investigation was facilitated.

References

1) GIESE, Peter: Die Bestimmung der elastischen Eigenschaften und der Mächtigkeit von Lockerböden mit Hilfe von speziellen Rayleigh-Wellen. Gerl. Beitr. Geophys., **66** (1957), 274–312.
2) TAZIME, Kyozi: Ray-theoretical Construction of Dispersive Rayleigh Waves. Journ. Phys. Earth, **6** (1958), 81–89.
3) TAZIME, Kyozi: Transition from Solid to Liquid Superficial Waves in a Plate. Journ. Phys. Earth, **6** (1958), 91–99.
4) TAZIME, Kyozi: Wave Groups Generated by a Very Small Explosion. Journ. Phys. Earth, **4** (1956), 113–126.
TAZIME, Kyozi: Relations between Charge Amounts and Periods in Resulting Seismic Wave Groups. Journ. Phys. Earth, **5** (1957), 51–59.
5) TOLSTOY, Ivan: Resonant Frequencies and High Modes in Layered Wave Guides. J. Acoust. Soc. Am., **28** (1956), 1182–1192.
TOLSTOY, Ivan and USDIN, Eugene: Wave Propagation in Elastic Plates. J. Acoust. Soc. Am., **29** (1957), 37–42.